พอลิไดเมทิลไซลอกเซนไมโครชิพสำหรับการตรวจวัดคอเลสเทอรอล

นางสาวนิภาพรรณ ฤาชา

วิทยานิพนธ์นี้เป็นส่วนหนึ่งของการศึกษาตามหลักสูตรปริญญาวิทยาศาสตรมหาบัณฑิต
สาขาวิชาปิโตรเคมีและวิทยาศาสตร์พอลิเมอร์
คณะวิทยาศาสตร์ จุฬาลงกรณ์มหาวิทยาลัย
ปีการศึกษา 2552

POLY(DIMETHYLSILOXANE) MICROCHIP FOR DETECTION OF CHOLESTEROL

Miss Nipapan Ruecha

A Thesis Submitted in Partial Fulfillment of the Requirements
for the Degree of Master of Science Program in Petrochemistry and Polymer Science
Faculty of Science
Chulalongkorn University
Academic Year 2009

Thesis Title	POLY(DIMETHYLSILOXANE) MICROCHIP FOR DETECTION OF CHOLESTEROL
By	Miss Nipapan Ruecha
Field of Study	Petrochemistry and Polymer Science
Thesis Advisor	Associate Professor Orawon Chailapakul, Ph.D.

Accepted by the Faculty of Science, Chulalongkorn University in Partial Fulfillment of the Requirements for the Master's Degree

……Dean of the Faculty of Science

(Professor Supot Hannongbua, Dr.rer.nat.)

THESIS COMMITTEE

…… Chairman

(Associate Professor Sirirat Kokpol, Ph.D.)

……. Thesis Advisor

(Associate Professor Orawon Chailapakul, Ph.D.)

…… Examiner

(Assistant Professor Warinthorn Chavasiri, Ph.D.)

…… External Examiner

(Weena Siangproh, Ph.D.)

นิภาพรรณ ฤาชา: พอลิไดเมทิลไซลอกเซนไมโครชิพสำหรับการตรวจวัดคอเลสเทอรอล (POLY(DIMETHYLSILOXANE) MICROCHIP FOR DETECTION OF CHOLESTEROL) อ.ที่ปรึกษาวิทยานิพนธ์หลัก: รศ.ดร.อรวรรณ ชัยลภากุล, 75 หน้า

งานวิจัยนี้เป็นการพัฒนาเพื่อตรวจวิเคราะห์คอเลสเทอรอลแบบรวดเร็ว โดยใช้เทคนิคไมโครชิพคะพิลลารีอิเล็กโทรฟอริซิสร่วมกับการวิเคราะห์โดยใช้เอนไซม์และตัวตรวจวัดทางเคมีไฟฟ้า ระบบสำหรับการวิเคราะห์โดยตรงแบบแอมเพอโรเมทรีในไมโครชิพคะพิลลารีอิเล็กโทรฟอริซิสถูกนำมาใช้ในวิเคราะห์หาปริมาณคอเลสเทอรอลได้เป็นอย่างดี อิทธิพลของความเข้มข้นและพีเอชของบัฟเฟอร์, ความเข้มข้นของเอนไซม์คอเลสเทอรอลออกซิเดส, ศักย์ไฟฟ้าที่ให้กับระบบ, เวลาที่ใช้ในการฉีดสารตัวอย่าง และศักย์ไฟฟ้าในการตรวจวัด ที่ใช้ในการวิเคราะห์ต่อค่าการตอบสนองของตัวตรวจวัดซึ่งได้ทำการตรวจสอบและหาค่าที่ทำให้เกิดประสิทธิภาพสูงสุดสำหรับการตรวจวัด จากผลการทดลองพบว่าสารไฮโดรเจนเปอร์ออกไซด์ที่เป็นผลผลิตสามารถตรวจวัดได้ในเวลาน้อยกว่า 100 วินาที เมื่อใช้ฟอสเฟตบัฟเฟอร์ความเข้มข้น 40 มิลลิโมลาร์ที่พีเอช 7.0, ความเข้มข้นของเอนไซม์คอเลสเทอรอลออกซิเดสที่ 0.68 ยูนิทต่อมิลลิลิตร, ศักย์ไฟฟ้าในการแยกที่ +1600 โวลต์, เวลาที่ใช้ในการฉีดสารตัวอย่างที่ 20 วินาที และศักย์ไฟฟ้าในการตรวจวัดที่ +0.5 โวลต์ โดยพบว่าพีดีเอ็มเอสไมโครชิพคะพิลลารีอิเล็กโทรฟอริซิสสามารถวิเคราะห์หาปริมาณคอเลสเทอรอลได้ในช่วงความเข้มข้นระหว่าง 38.7 ไมโครกรัมต่อเดซิลิตร (1 ไมโครโมลาร์) ถึง 270.6 มิลลิกรัมต่อเดซิลิตร (7 มิลลิโมลาร์) โดยมีขีดจำกัดต่ำสุดของการตรวจวัดเป็น 38.7 นาโนกรัมต่อเดซิลิตร ในงานวิจัยนี้แสดงให้เห็นถึงระบบของไมโครชิพคะพิลลารีอิเล็กโทรฟอริซิสที่สามารถนำไปประยุกต์ใช้ในการวิเคราะห์หาปริมาณคอเลสเทอรอลในตัวอย่างซีรัม เปอร์เซนต์การคืนกลับอยู่ในช่วง 98.9 เปอร์เซนต์ ถึง 101.8 เปอร์เซนต์ พีดีเอ็มเอสไมโครชิพคะพิลลารีอิเล็กโทรฟอริซิสควบคู่กับการวิเคราะห์โดยใช้เอนไซม์ร่วมกับตัวตรวจวัดทางเคมีไฟฟ้าเป็นเทคนิคที่มีความรวดเร็วและไวสำหรับการวิเคราะห์คอเลสเทอรอล

สาขาวิชา ปิโตรเคมีและวิทยาศาสตร์พอลิเมอร์ ลายมือชื่อนิสิต .....

ปีการศึกษา 2552 ลายมือชื่อ อ.ที่ปรึกษาวิทยานิพนธ์หลัก .....

5072327523: MAJOR PETROCHEMISTRY AND POLYMER SCIENCE
KEYWORDS: CHOLESTEROL/ CHOLESTEROL OXIDASE/ MICROCHIP CAPILLARY ELECTROPHORESIS/ POLY(DIMETHYLSILOXANE)

NIPAPAN RUECHA: POLY(DIMETHYLSILOXANE) MICROCHIP FOR DETECTION OF CHOLESTEROL. THESIS ADVISOR: ASSOC. PROF. ORAWON CHAILAPAKUL, Ph.D., 75 pp.

In this work, the rapid detection of cholesterol using poly(dimethylsiloxane) microchip capillary electrophoresis, based on the coupling of enzymatic assays and electrochemical detection, was developed. Direct amperometric detection for poly(dimethylsiloxane) (PDMS) microchip capillary electrophoresis was successfully applied to quantify cholesterol levels. Factors influencing the performance of the method (such as the concentration and pH value of buffer electrolyte, concentration of cholesterol oxidase enzyme, separation voltage, injection time, and detection potential) were carefully investigated and optimized. The migration time of hydrogen peroxide, product of the reaction, was less than 100 s when using 40 mM phosphate buffer at pH 7.0 as the running buffer, a concentration of 0.68 $U.mL^{-1}$ of the cholesterol oxidase enzyme, a separation voltage of +1600 V, an injection time of 20 s, and a detection potential of +0.5 V. PDMS microchip capillary electrophoresis showed linearity between 38.7 $\mu g \cdot dL^{-1}$ (1 μM) and 270.6 $mg \cdot dL^{-1}$ (7 mM) for the cholesterol standard; the detection limit was determined as 38.7 $ng.dL^{-1}$. To demonstrate the potential of this assay, the proposed method was applied to quantify cholesterol in serum samples. The percentages of recoveries were assessed over the range of 98.9 % to 101.8 %. Therefore, PDMS microchip capillary electrophoresis, based on the coupling of enzymatic assays and electrochemical detection, is very rapid and sensitive method for the determination of cholesterol levels.

Field of Study: Petrochemistry and Polymer Science Student's Signature .....

Academic year: 2009 Advisor's Signature .....

CONTENTS

PAGE

PAGE

PAGE

PAGE

PAGE

LIST OF TABLES

TABLES **PAGE**

LIST OF FIGURES

FIGURES **PAGE**

FIGURES **PAGE**

FIGURE **PAGE**

FIGURE **PAGE**

FIGURE **PAGE**

LIST OF SCHEMES

SCHEME **PAGE**

LIST OF ABBREVIATIONS

ChOx	Cholesterol oxidase enzyme
MCE	Microchip capillary electrophoresis
PDMS	Poly(dimethylsiloxane)
CE	Capillary electrophoresis
HPLC	High performance liquid chromatography
UV	ultraviolet
μ_{EP}	electrophoretic mobility
EOF	electroosmotic flow
ν	migration velocity
E	applied field
r	ionic radius
q	net charge
F_e	electric force
F_f	countering friction force
ε	dielectric constant
η	viscosity of the buffer
ζ	zeta potential of the liquid-solid interface
CZE	capillary zone electrophoresis
IUPAC	International Union for Pure and Appiled Chemistry
Q	number of coulombs
N	moles of material
n	number of electron equivalent lost
F	Faraday's constant
i	respect to current
i_d	directly proportional
δ	thickness of the diffusion layer
E_p	peak potential

i_p	peak current
$i_{p,a}$	anodic peak current
$E_{p,a}$	anodic peak potential
$i_{p,c}$	cathodic peak current
$E_{p,c}$	cathodic peak potential
A	electrode area
D	diffusion coefficient
μm	micrometer
cm	centimeter
mm	millimeter
m	meter
s	second
V	voltage
mol	mole
C	concentration of electroactive species ($mol \cdot cm^3$)
ν	scan rate ($V \cdot s^{-1}$.)
B	buffer reservoir
W	waste reservoir
S	sample reservoir
SW	sample waste reservoir
HV	high voltage
N	plate number
σ^2	spatial variance of a zone
L	migrating a distance
PET	polyethylene terephthalate
PC	polycarbonate
PMMA	poly(methyl methacrylate)
K	degree Kelvin
Pa	Pascal
°C	degree Celsius
LIF	laser-induced fluorescence
MS	mass spectrometry

CL	chemiluminescence
LDL	low density lipoprotein
HDL	high density lipoprotein
mg	milligram
dL	deciliter
M	molarity (mol/L)
LOD	limit of detection
LOQ	limit of quantitation
SD	standard deviation
RSD	relative standard deviation
PB	phosphate buffer
MES	2-morpholinoethanesulfonic acid monohydrate
U	unit
Au	gold

CHAPTER I

INTRODUCTION

1.1 Introduction

One of the most important and frequently quantified substrates in clinical analysis is the blood cholesterol. Cholesterol is a steroid metabolite of waxy nature constituting an essential of mammalian cell membranes and is transported in the blood plasma of all animals. In addition, cholesterol is an important component in the manufacture of bile acids, steroid hormones, and several fat-soluble vitamins. A high level of cholesterol level in the blood is a major risk for coronary heart disease [1-2].

The conventional method for the determination of cholesterol utilizes the reaction between cholesterol and cholesterol oxidase enzyme (ChOx), and hydrogen peroxide produced is detected by spectrophotometry [3-5]. However, this technique is not suitable for rapid analysis or for cost effective detection because it follows a complicated principle and requires an expensive instrument as well as reagents. As an alternative, amperometric biosensors [6-10] have been proposed based on the immobilization of cholesterol oxidase enzyme with respect to the cholesterol reaction sequence. Unfortunately, various matrix species such as ascorbic acid, interfere with these biosensors.

In the past decade, microfluidic biosensor [11-28] chips have been developed for medical and biological applications. Enzyme sensor chips based on electrochemical detection are widely studied by many researchers. However, almost all the studies focus on the fabrication of small electrodes and chambers as well as the possibility of applying the optimized method to the fabrication of micro devices by immobilizing the enzyme on the surface of the electrode and on chips. Microchip capillary electrophoresis (MCE) has been developed for the separation of biological compounds including DNA and proteins [29-30]. MCE is technique that integrates with laboratory functions on a single chip. MCE is promising alternative for the determination of cholesterol because it is easy to use, require small volumes of

reagents and sample, and provide rapid analysis. Moreover, electrophoretic separation in MCE is an efficient way to minimize the matrix effect by the specific migration time of the analyte.

The general material for microchip fabrication is glass [11-17], such as quartz and borosilicate, but the method of glass fabrication is complicated and relatively difficult for fabrication. Poly(dimethylsiloxane) (PDMS) [18-21] is an attractive material for microchip fabrication due to its excellent optical transparency, easy replica molding, non-toxicity and biocompatibility. Consequently, PDMS has become popular for in the manufacture of microchip devices. The current detection methods for MCE are laser-induced fluorescence detection [22-24], absorbance detection [25], and amperometric detection [11-21,26]. Among these detection schemes, amperometric detection is an attractive choice for the microchip systems given its high sensitivity, and miniaturized instrumentation. The aim of this work was to carry out bioanalytical assays based on enzymatic reactions for diagnostic applications, by combining the attractive performance of MCE and the high sensitivity of electrochemical principles.

In this thesis, PDMS microchip capillary electrophoresis coupled with electrochemical detection, based on an enzymatic reaction and electrophoretic separations was developed for the rapid detection of cholesterol. Cholesterol and the ChOx enzyme reagent were flow through the separation channel; then the sample was introduced to mix at the channel intersection and in the separation channel using electrokinetic flow. The hydrogen peroxide produced from the enzymatic reaction was immediately detected at the downstream gold wire working electrode.

1.2 Research objectives

The two main goals of this thesis are as follows:

1. To determine the optimal conditions of the PDMS microchip capillary electrophoresis coupled with amperometry for the quantification of cholesterol.
2. To apply the proposed system for the fast determination of cholesterol level in serum samples.

1.3 Scopes of investigation

In this work, PDMS microchip capillary electrophoresis was first prepared and characterized. Then, the factors affecting the performance of the PDMS microchip (such as, the effect of concentration and pH of background electrolytes, the effect of detection potential, the effect of cholesterol oxidase enzyme, the effect of separation voltage, and the effect of injection time) were studied with respect to the detection of cholesterol. A gold wire electrode was employed; both the analytical recovery and the precision of the method were investigated. The successful application of PDMS microchip capillary electrophoresis coupled with electrochemical detection to serum samples is reported in the next section of this thesis.

CHAPTER II

THEORY AND LITERATURE SURVEY

In this chapter, the fundamentals of capillary electrophoresis are discussed. In the second part of this chapter, aspects of microchip capillary electrophoresis and electrochemical detection are treated. The discussions in this chapter refer to the basic principles of microchip used in the subsequent chapters.

2.1 Fundamentals of capillary electrophoresis

Capillary electrophoresis is rapidly maturing as a major technique for the analysis of proteins, nucleic acid, and biomarkers. Capillary electrophoresis (CE) is a novel and alternative format for both liquid chromatography [32]. The unique properties of this technique inclued the use of

- Capillary tubing in the range of 25-100 μm;
- High electric field strength;
- On-line detection in real time;
- Limited quantities of mostly aqueous reagents; and
- Inexpensive capillaries compared to expensive HPLC column

The basic instrumental configuration for CE is relatively simple: a fused-silica capillary with an optical viewing window, a controllable high voltage power supply, two electrode assemblies, two buffer reservoirs, and an ultraviolet (UV) detector are required. The ends of the capillary are placed in the buffer reservoirs, and the optical viewing window is aligned with the detector. After filling the capillary with buffer, the sample can be introduced by first dipping the end of the capillary into the sample solution and then by elevating the immersed capillary a foot or so above the detector side buffer reservoir. While relatively easy to use for experimentation, these early CE systems were inconvenient for routine analysis and too imprecise for quantitative analysis. Compared to the earlier instruments, this fully automated version offers computer control of all operations, such as pressure and electrokinetic injection, an autosampler and fraction collector, automated methods development, precise

temperature control, and an advanced heat dissipation system. Automation is critical to CE since repeatable operation is required for precise quantitative analysis [31-34].

2.1.1 Electrophoretic Mobility

The movement (migration) of a charge species under the influence of an applied field is characterized by its electrophoretic mobility (μ_{EP}) whose units are $cm^2.sec^{-1}.V^{-1}$. Mobolity depends not only on the charge density of the solute but also on the dielectric constant and viscosity of the electrolyte. Mobility is also strongly dependent on temperature. The separation of ions is facilitated by the use of high voltages, which may generate both an electroosmotic flow (EOF) and an electrophoretic flow of buffer solutions and ionic species, within the capillary. All particles in the stream of buffer moving under the influence of an electric field are carried along by the EOF. The mobility of ions in a solution is governed by their charge-to-size ratio while the size of molecule is based on its molecular weight [30,32].

The migration velocity (ν) of solute molecules is proportional to the applied field (E) and the electrophoretic mobility (μ_{EP}) according to the following equation:

$$\nu = \mu_{EP} + E \qquad \text{(Equation 2.1)}$$

The electrophoretic mobility depends on the ionic radius (r) and net charge (q) of the molecule and assume a constant velocity where the electric force (F_e) is balanced by the countering friction force (F_f) such that $Fe = F_f$

$$Fe = q \,.\, E \qquad \text{(Equation 2.2)}$$

$$F_f = 6\pi\eta r\nu \qquad \text{(Equation 2.3)}$$

Ionic size modifies mobility because of the solute's exposure to frictional drag as it migrates through the supporting electrolyte. The frictional drag is directly proportional to viscosity, size, and electrophoretic velocity. An expression for mobility is given below:

$$\mu_{EP} = \frac{\nu}{E} = \frac{q}{6\pi\eta r} \qquad \text{(Equation 2.4)}$$

Fundamental to any CE plateform utilizing a mobile carrier solution, an externally applied field produces two independent and distinguishable flow parameters in response to electroosmotic mobility (μ_{EOF}) namely the migration of charged analyte molecules suspended in the buffer solution, or the electrophoretic mobility (μ_{EP}), both of which are established in response to the field. While the anions are attracted to the anode, they do not actually move towards it, but simply resist the effects of the EOF. The total mobility and corresponding flow of the analytes migrating in the channel is the sum of the electroosmotic and electrophoretic flow. However, the predominating value is the EOF, which is directed towards the cathode. The sum of the two mobilities yields μ_{AAP}, which is the apparent mobility of the analyte as shown in Equation 2.5 and Figure 2.1

$$\mu_{AAP} = \mu_{EOF} \pm \mu_{EP} \qquad \text{(Equation 2.5)}$$

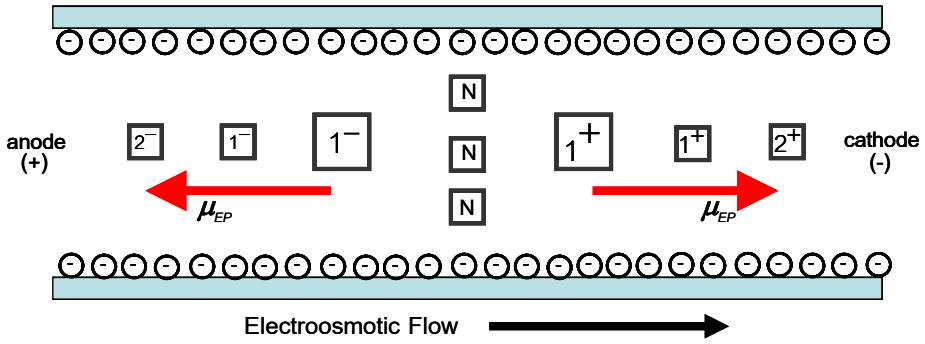

Figure 2.1 Representation of effective mobilities for N neutral species, negatively species, and positively species.

Separation by size does occurs to a small extent in CE. However, this effect is negligible for small analytes, whose hydrated molecular shell is subjected to very little drag while moving under the influence of the electric field. For the extremely large molecules like proteins, where the charge-to-size ratio is considerably different from smaller molecules for example, this drag force would become significant and

would have to be considered. The typical order of elution of positive, negative, and neutral molecules in the background electrolyte is outlined in Figure 2.2.

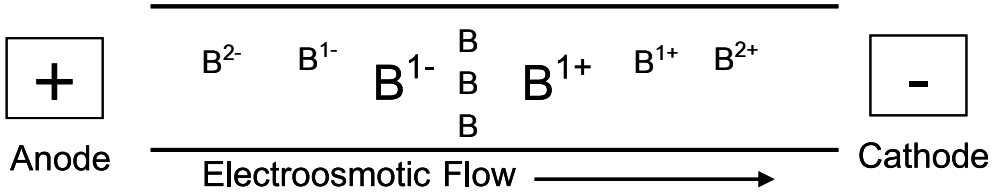

Figure 2.2 Representation of positive charge species, negative charge species, and neutral species distribution in an electrophoretic separation including representation for separation by size.

2.1.2 Electroosmotic flow

Electroosmotic flow (EOF) is the term used to describe the movement of a liquid in contact with a solid surface when a tangential electric field is applied. EOF is often used, when flowing in the same direction as the analytes, to increase the speed with which the analytes reach the detector or, when flowing in the same direction as the analytes or to improve resolution when following in the opposite direction of the analytes [35].

EOF occurs in fused silica capillaries because acidic silanol group at the surface of the capillary dissociate when in contact with an electrolyte solution according to the following equation:

$$SiOH\ (s) \rightleftharpoons SiO^{-}\ (s) + H^{+}\ (aq)$$

Hydrate cations in the electrolyte solution are attracted to the negatively charged silanol groups and become arranged into two layers. As illustrated in Figures 2.3 and 2.4, one layer is tightly bond by electrostatic forces (compact layer), and the other is more loosely bond (diffuse layer). When an electric field is applied, the diffuse layer breaks away at the plane of shear and moves towards the cathode, dragging with it the bulk solution of the electrolyte, as a result of viscous drag. This flow of bulk solution is known as electroosmosis.

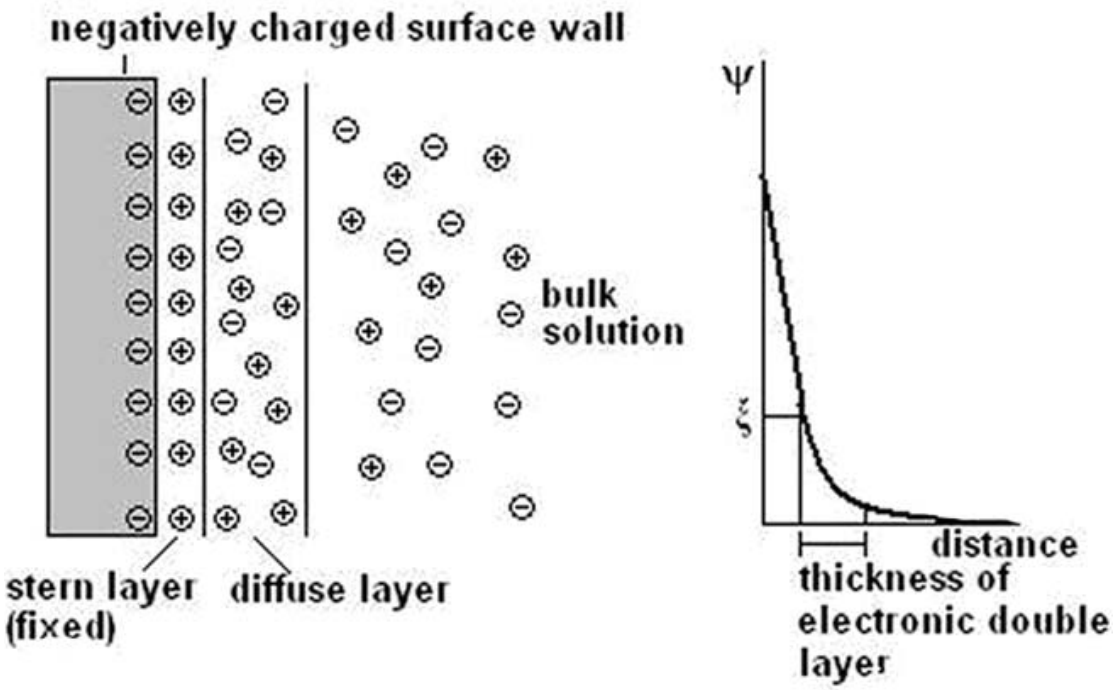

Figure 2.3 The electric double layers formed next the negative charged solid surface.

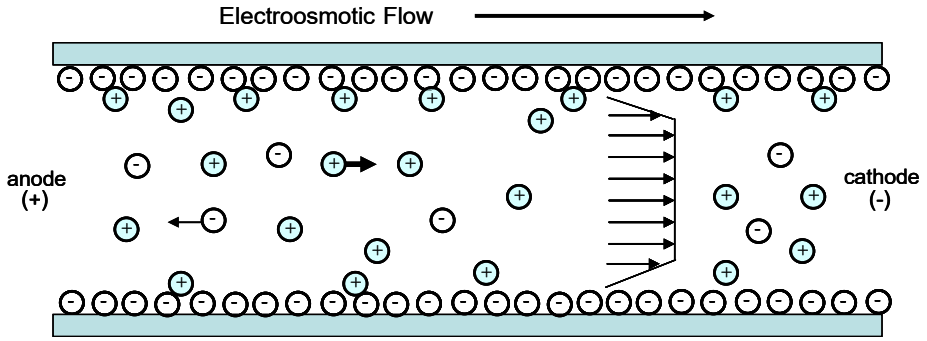

Figure 2.4 Electroosmotic velocity profile in microchannel.

Further from the wall, a compact and mobile solution becomes electrically neutral as the zeta potential of the wall is no longer sensed. When a voltage is applied, the mobile positive charges migrate in the direction of the cathode (the negative electrode). Science ions are solvated by water, the fluid in the buffer is mobilized as well and dragged along by the migrating charge. Although the double

layer is approximately 100 Å thick, the EOF is transmitted throughout the diameter of the capillary, presumably through hydrogen bonding of water molecules or by van der Waals interactions between the buffer constituents [32].

The EOF as defined by

$$\nu_{eo} = \frac{\varepsilon\zeta}{\eta} E \qquad \text{(Equation 2.6)}$$

where ε is the dielectric constant, η is the viscosity of the buffer, and ζ is the zeta potential of the liquid-solid interface. The equation is only valid for the capillaries that are sufficiently large such that the double layers on the opposite walls do not overlap each other. Practical use of this equation is not forthcoming, as the zeta potential is rarely measured and data for the dielectric constants of mixtures are not readily available. Like electrophoretic mobility, the EOF is inversely proportional to the viscosity of the background electrolyte.

2.1.3 Separation Efficiency

The EOF affects to the amount of time a solute resides in the capillary; both the separation efficiency and resolution are related to the direction and flow of the EOF. The EOF profile shown in Figure 2.5, is compare with hydrodynamic flow. The EOF profile will not be parabolic as in the hydrodynamic flow, where drag from stationary surface slows the liquid at the walls. Instead the flow profile is flat and produced less band broadening than a parabolic flow profile from the hydrodynamic flow.

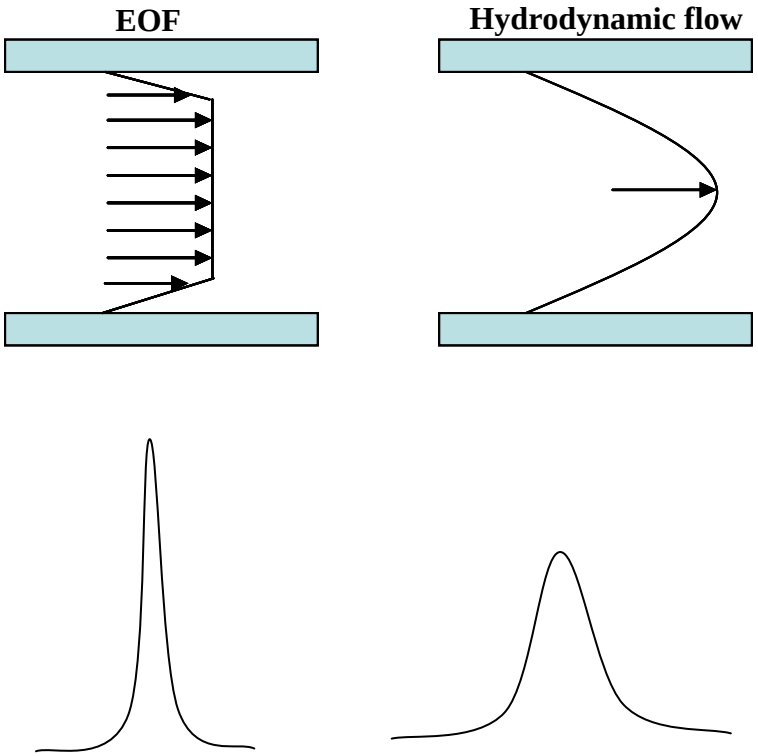

Figure 2.5 Flow profile and effect on peak shapes for electroosmotic flow and laminar flow.

2.1.4 Separation mode in capillary electrophoresis

In capillary electrophoresis, a sample (usually containing charged species) is introduced into the end of a capillary that has been filled with a solution of buffer. Under the influence of an electric field, the analytes migrate away from the injection end of the capillary toward the detector end, where they are visualized.

The first and most often encountered separation mechanism in CE is based on mobility differences of the analytes in an electric field; these differences are dependent on the size and charge to mass ratio of the analyte ion. Analyte ions are separated into distinct zones when the mobility of one analyte differs sufficiently from mobility of next. This mechanism is exemplified by capillary zone electrophoresis (CZE).

CZE is the simplest and most widely used mode in CE. Separations take place in an open-tube fused silica capillary under the influence of an electric field. The velocity of the analytes is modified by controlling the pH, viscosity, or concentration

of the buffer, or by changing the separation voltage. The EOF is often used in this mode to improve resolution or to shorten analysis times. In CZE, the composition of the electrolyte is constant in the capillary and the reservoirs surrounding the two electrodes. The electrolyte provides an electrically conducting and buffering medium. Upon introduction of a sample, each species of analyte ions migrates in the buffer in a discrete zone and at a different velocity from the other species. Neutral molecules are carried along by the EOF as a single, unresolved peak. Owing to the presence of the EOF, both anions and cations can be seen in a single run. However, separations are usually optimized for one species or the other [36]. This mechanism is illustrated in Figure 2.6.

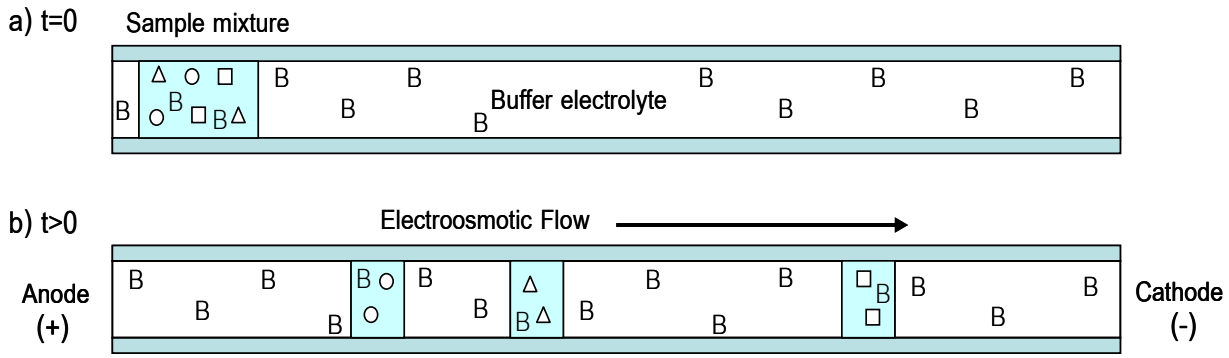

Figure 2.6 Separation mechanism in CZE, where B represents buffer, a) Sample mixture is introduced into capillary; b) voltage is applied, and the analytes separate into distinct zones.

The application of CZE is very useful for the separation of proteins and peptides since complete resolution can often be obtained for analytes differing by only one amino acid substituent. This is particularly important in tryptic mapping where mutations and post-translational modifications must be detected. Other applications where CZE may be useful include the separation of inorganic anions and cations such as those typically separated by ion chromatography. Small molecules such as pharmaceuticals can often be separated unless they are charged. In most cases, the technique of micellar electrokinetic capillary chromatography yields superior results for charged as well as neutral small molecules.

2.1.5 Stacking in capillary zone electrophoresis

Stacking is one of the desirable features of CE which has not been fully explored or utilized. Stacking in CE is similar to sample enrichment in HPLC. However, from a practical point of view, it is easier to perform stacking in CE relative to sample enrichment in HPLC. There is no need for complicated steps or special equipment in CE. Stacking can be achieved using several different principles but requires careful planning. Here, the mechanism and the different methods to achieve stacking in capillary zone electrophoresis (CZE) for different types of compounds are reviewed with several examples. Some of these methods are easier to perform or more suited for certain applications than others [37,38].

The basic principle of sample stacking of anions is summarized in Figure 2.7. The region containing the sample ions is a low conductivity solution while the background region is a high conductivity solution (Figure 2.7 A). If a low and a high conductivity solution are present inside a capillary, upon the application of voltage, the low conductivity region will experience a higher electric field compared to the background region. Sample ions will then move faster in the low conductivity region than in the high conductivity region. The abrupt change in sample ion movement across the concentration boundary then results in the reduction of sample zone length, hence creating zones with concentrations higher than the original (Figure 2.7 B). The electroosmotic flow (EOF) is assumed to be zero here [37, 38].

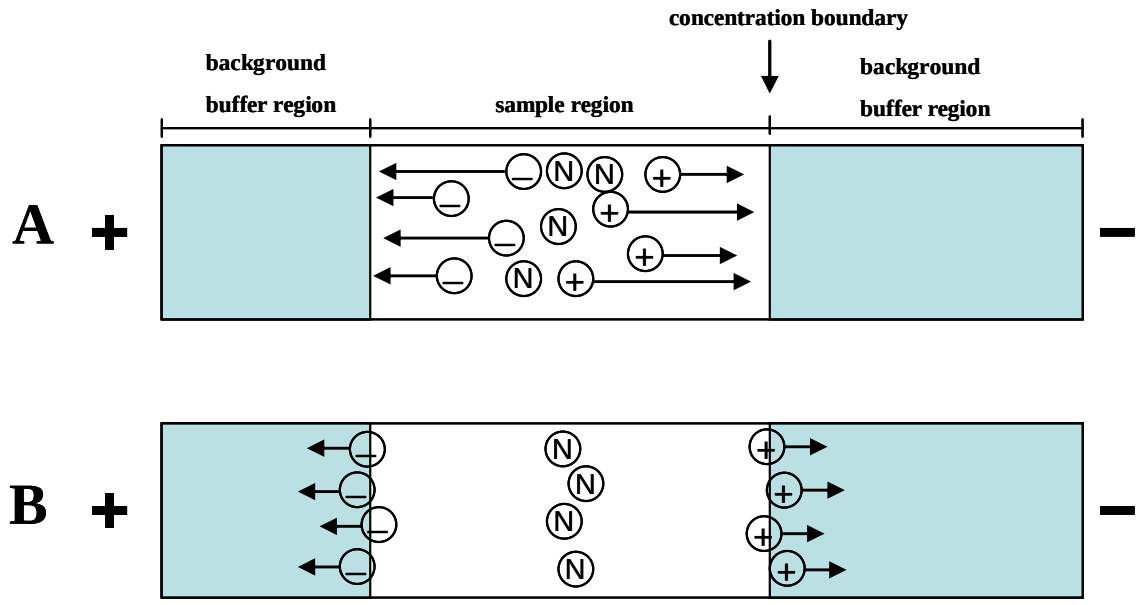

Figure 2.7 General sample stacking model for anions. Discussion is found in the text [37].

2.2 Electroanalytical Method

Electrochemical techniques are classified by the International Union for Pure and Applied Chemistry (IUPAC) on the basis of their working principles. The different classes of electrochemical techniques are electrolytic, potentiometric, conductometric, polarographic or voltammetric, amperometric, impedimetric, and coulometric methods. In potentiometry, measurements are based on the equilibrium potential existing between a selective electrode and a reference electrode. The detection limit of this technique is in the micromolar range. However, the detection limit of voltametry is better than that of potentiometry; as a result the latter technique can be used precisely for trace analysis. Although many electrochemical methods are available, only amperometry and cyclic voltammetry are used in this thesis [39,44].

2.2.1 Amperometry

Amperometry is a one technique of electrochemical detection, where the potential of the working electrode is constant and the current is detected as a function of time as shown in Figure 2.8. Amperometry usually is carried out in stirred or flowing solutions or at the working electrode. The potential of a chosen working electrode with respect to the reference electrode is set at a fixed potential to detect the change in the current response. At this potential, the electroactive species undergo either oxidation or reduction at the electrode [40-43].

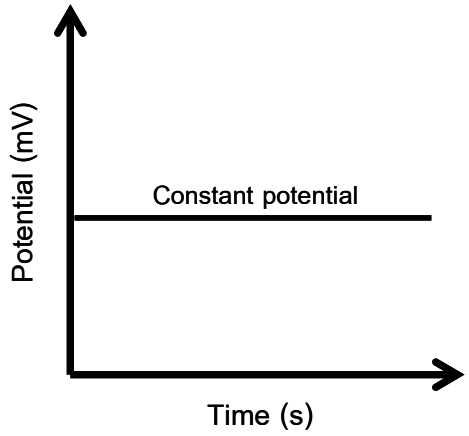

Figure 2.8 A typical waveform employed in amperometry.

All amperometric determination ultimately depends upon Faraday's law

$$Q = nFN \qquad \text{(Equation 2.6)}$$

where Q is the number of coulombs used in converting N moles of material, n is the number of electron equivalent lost or gained in the transfer process per mole of material, and F is Faraday's constant. Q is related to the current, i as follows:

$$\frac{dQ}{dt} = i = nFA\frac{dN}{dt} \qquad \text{(Equation 2.7)}$$

and mass transfer is given by

$$\frac{dN}{dt} = -D\left(\frac{dC_{x,t}}{dx}\right)_{x=0} \qquad \text{(Equation 2.8)}$$

Under controlled hydrodynamic conditions, the rate of the whole process is controlled by diffusion mass transfer. The diffusion current, i_d is directly proportional to the concentration of the electroactive substance, C:

$$i_d = nFAD\frac{C}{\delta} \qquad \text{(Equation 2.9)}$$

where δ is thickness of the diffusion layer (which is constant at a given convection). A low detection limit and wide linear measuring range are the main advantages of amperometric techniques.

The amperometric current is a function of the number of the molecules or ions that have been removed by the reaction at the electrode. Thus, the resultant amperometric signal is directly proportional to the concentration of the analyte [39,44].

2.2.2 Cyclic voltammetry

Cyclic voltammetry is a completed voltage scan (y axis) versus time (x axis) in forward and backward directions, as shown in Figure 2.9. The voltage scan reverses direction after the maximum current of the forward process has passed. The backward scan gives a signal in the opposite direction from the forward scan. This technique provides information about the properties and characteristics of the electrochemical process and also provides insight into any complicating side processes (such as pre- and post-electron transfer reactions), as well as kinetic considerations [39,44].

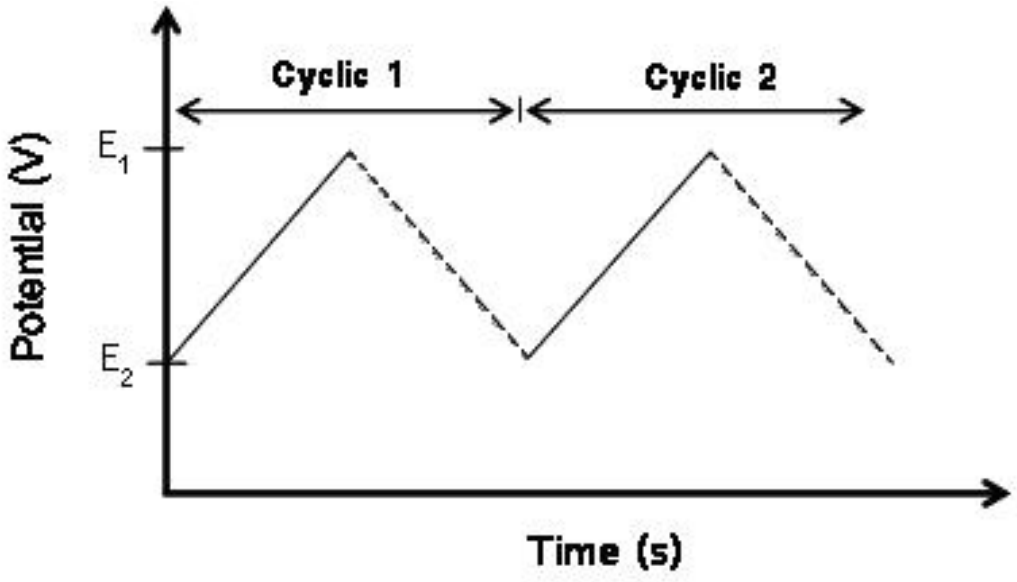

Figure 2.9 Potential-time profiles used for cyclic voltammetry. Solid line represents forward scan and dashed line represents backward scan.

Voltammetry measurements was characterized by a peak potential, E_p, at which the current reaches its maximum value; that value is called the peak current, i_p. The $i_{p,a}$ and $E_{p,a}$ are the anodic peak current and anodic peak potential, respectively. The $i_{p,c}$ and $E_{p,c}$ are the cathodic peak current and cathodic peak potential, respectively. The shape of a reversible cyclic voltammogram with an electrode of fixed area is shown in Figure 2.10

The peak current is given by the Randles-Sevcik equation below:

$$i_p = 2.69\times10^5 n^{3/2} A D^{1/2} C \nu^{1/2} \text{ at } 25°C \qquad \text{(Equation 2.10)}$$

where i_p is in A, A (electrode area) is in cm^2, D (diffusion coefficient) is in $cm^2 \cdot s^{-1}$, C (concentration of electroactive species) is in $mol \cdot cm^3$, and ν (scan rate) is in $V \cdot s^{-1}$.

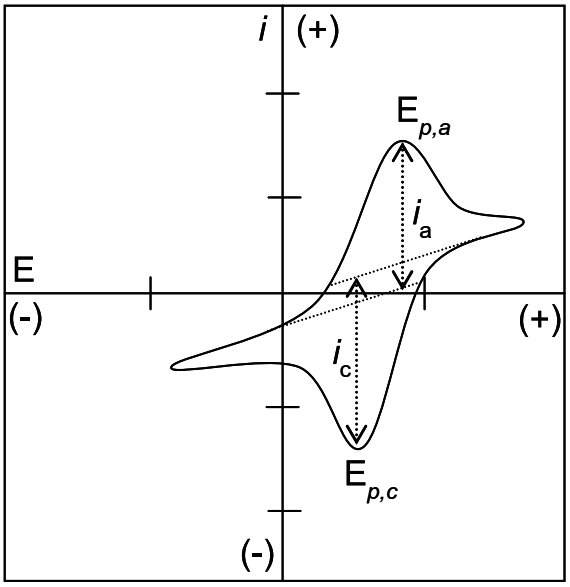

Figure 2.10 Typical reversible cyclic voltammetry with the initial sweep direction towards more positive potential.

A useful parameter of the voltammetric curve is the half-peak potential, $E_{p/2}$, which is the potential at which the registered current reaches half of its maximum value, it is used to characterize a voltammogram. For a reversible process, $E_{1/2}$, is located halfway between E_p, and $E_{p/2}$. The ratio of the peak current for the cathodic process relative to the peak current for the anodic process is equal to one ($i_{p,c}/i_{p,a} = 1$). To measure the peak current for the cathodic process, the extrapolated baseline going from the foot of the cathodic wave to the extension of this cathodic current beyond the peak must be used as a reference, as illustrated in Figure 2.11. The difference in the peak potentials between the anodic and cathodic processes of the reversible reaction is given by the equation below:

$$|\Delta E_p| = |\Delta E_{p,a} - \Delta E_{p,c}| = \frac{0.059}{n} \qquad \text{(Equation 2.11)}$$

This provides a rapid and convenient means of determining the number of electrons involved in the electrochemical reaction. For a reversible system, i_p is a linear function of $\nu^{1/2}$, and E_p is independent of ν.

2.3 Microchip capillary electrophoresis

Microchip capillary electrophoresis (MCE), also known as a microfluidics device or lab on a chip refers to a set of technologies that control the flow of minute amounts of liquids or gases in a miniaturized system, because it is a fluid-base handling method. MCE was primarily introduced by analytical chemists in need of microchemical analysis platforms; it is often coupled with laser excitation of molecular probes and fluorescent detection schemes. MCE systems have shown potential in a diverse array of biological applications, including biomolecular separations [45-47], enzymatic assays [48-49], the polymerase chain reaction [50-51], and immunohybridization reactions [52-53]. An important development in shrinking the size scale of fluidics was the use of electrokinetic flow to drive fluids in channels defined by microlithography and etching processes. More recently, this technology has been extended to nanoscale dimensions to manipulate individual molecules. MCE has developed rapidly in the past decade, and many products have become commercially available. Additionally, many companies using platforms to perform chemical analysis. In the life sciences, MCE could realize increases in efficiency of several order of magnitude. Samples volumes and assay times are reduced, thereby decreasing costs. Applications include biological and chemical analysis, pressure sensing, capillary electrophoresis, flow-based separations, fluid control for diagnostic microarrays, PCR amplification, DNA analysis, cell patterning, and drug delivery. MCE has enabled the acceleration of DNA hybridization times and resulted in quicker analysis. MCE enabled the use picomole amounts of peptide for analysis by mass spectrometry. Also, MCE has led to advances in tissue engineering, allowing for better oxygen flow and waste removal. Overall, MCE offers the possibility of solving large-scale system integration issues for biology and chemistry.

2.3.1 Microchip design

MCE may be carried out on miniaturized analytical devices. In this approach, the column of MCE is replaced with a microchip with a much shorter channel length and smaller dimensions, which offers dramatically shorter in analysis times and reduces reagent consumption.

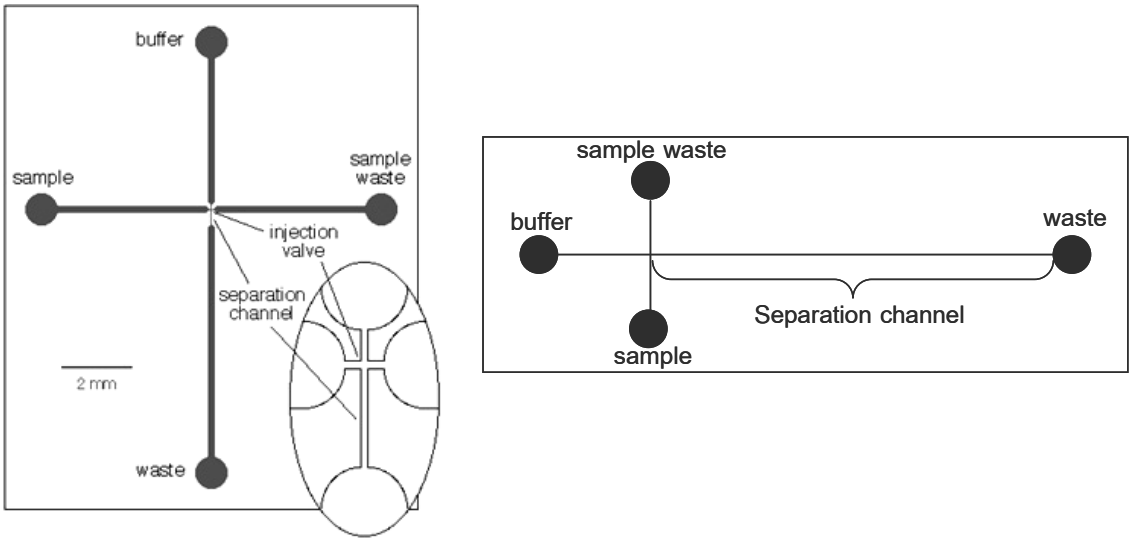

Figure 2.11 Illustrative examples of different layout of MCE.

2.3.2 Injection mode

One of the differences between MCE and conventional CE is the method by which the sample plug is introduced into the capillary. In conventional instruments, one end of the capillary is immersed in the sample solution. Then, the sample is driven into the capillary by applying a pressure pulse (hydrodynamic injection) or using EOF (electrokinetic injection). For microchip separation, a very short sample plug (<1 mm) needs to be introduced. To permit this, MCE typically employs a column coupling configuration of channels as shown in Figure 2.12. In the cross injector design and double-T in Figure 2.12, A and B are among the earliest designs employed in MCE [30].

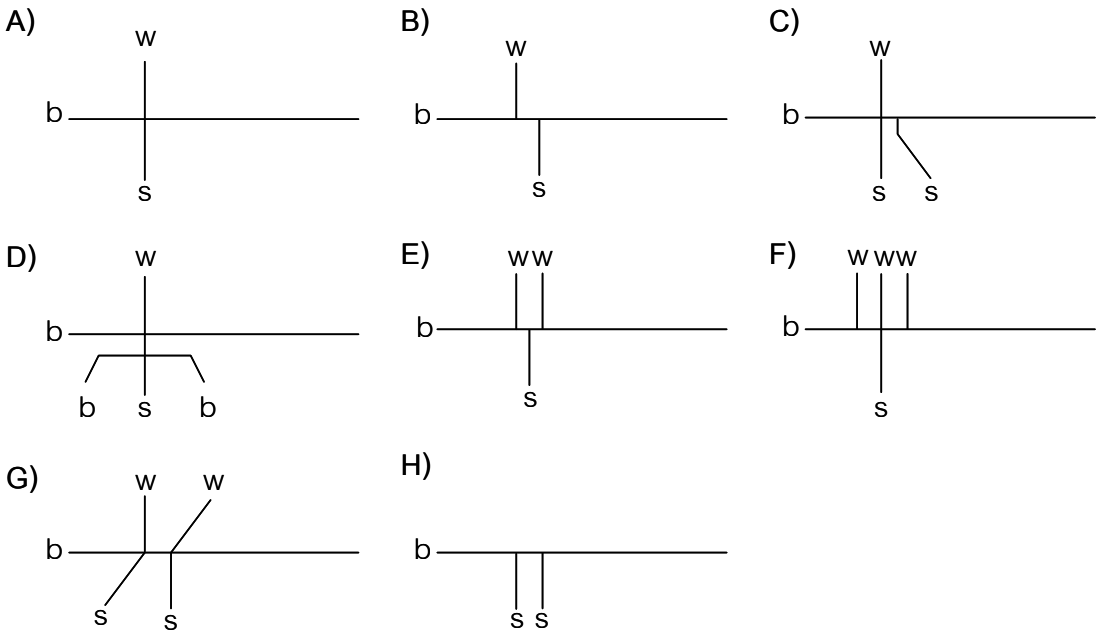

Figure 2.12 Examples of sample injector types. A) cross, B) double-T, C) double-L, D) double cross, E) triple-T, F) multi-T, G) stacking type, and H) π-injector. Sample inlet s, waste w and BGE inlet b are indicated [20].

2.3.2.1 Gated injection

The principle of the gated injection is shown in Figure 2.13. The main waste reservoir at the end of the injection channel is set to the ground at all times. The settings are same in pre-injection and run mode. Voltages are set so that the mobile phase will flow from the buffer reservoir (B) to the waste reservoir (W), and the sample will run from the sample reservoir (S) to the sample waste reservoir (SW). To prevent any sample from bleeding into the separation channel, the voltage on B is set higher than the voltage on S so that some mobile phase will always run into the SW [20].

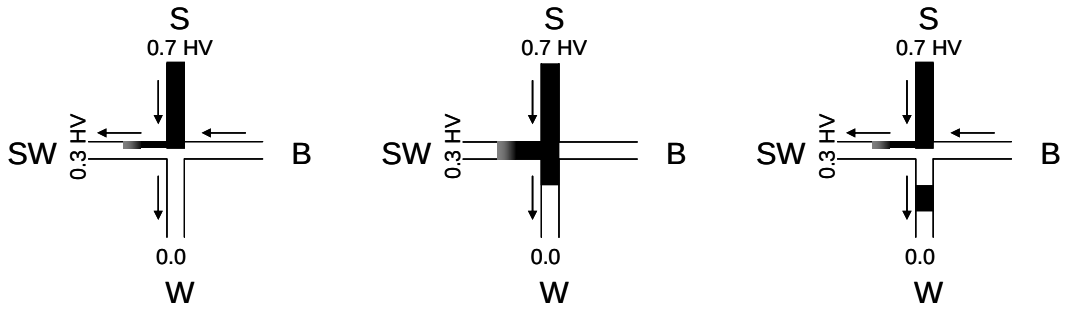

Figure 2.13 Principle of gated injection. Black stream is the sample, and white stream is the mobile phase. S: sample, SW: sample waste, B: buffer, and W: waste.

In the injection mode, B and SW are set to float, ensuring that no current will run through either reservoir. As a result no fluid will flow to or from either reservoir. The voltage on S and W are the same as those in the run mode, so a plug of sample will flow into the separation channel as long as the voltages are in the injection settings. Typically, the injection mode is switched. Gated injection is very simple to perform, and it allows for injection as long as necessary into the separation channel; however the drawback of this mode is bias in the injection. A sample plug injected into the cation sample plug will be slightly longer than for neutral species, and an anion sample plug will be slightly shorter than for neutral species.

2.3.2.2 Pinched injection

The principle of gated injection is shown in Figure 2.14. The sample is placed on one of the side-arms of the cross, the mobile phase is placed in the top reservoir, and the sample waste is placed on the other side-arm. The waste reservoir needs to be filled with fresh mobile phase. In the load position samples flow from S toward SW, over the cross. The mobile phase flows from both B and W to SW to prevent bleeding of the sample into the main channel. The sample stream is pinched together by the two mobile phase streams. In the run position, the voltages are switched so that the mobile phase will flow from B to the cross and towards all three reservoirs. Most of the flow is directed toward the separation column to drive the sample plug forward, but some mobile phase flow will also be directed towards S and SW

bleeding. The size of the sample plug is determined by geometry of the injection cross, so that its length can never be more than the width of the channels at the injection cross. However, the sample plug can be made smaller. By increasing the amount of buffer from B and W, the pinched sample stream at the junction becomes narrower, and a shorter plug is injected [20].

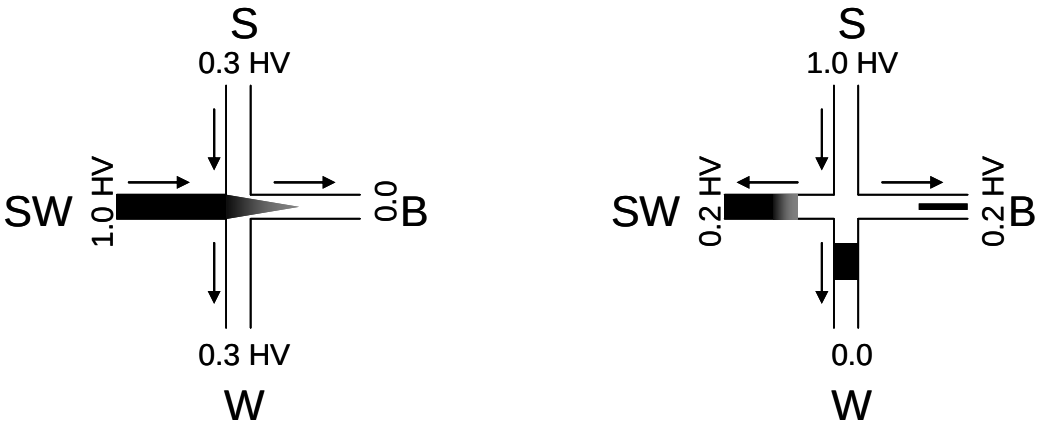

Figure 2.14 Principle of pinched injection. Black stream is the sample, and white stream is the mobile phase. S: sample, SW: sample waste, B: buffer, and W: waste.

As long as the loading step in the pinched injection is given sufficient time, there is no bias in the sample injected, as in the gated injection. A drawback of using the pinched injection is that after each run, the microchip needs to switch to the load position and needs to equilibrate before a new run is possible. Another disadvantage of the pinched injection is that the load position has a backflow of mobile phase from the W reservoir, which will contain some analytes after a few runs. Therefore, the separation channel will fill up with analytes during this backflow. Because the sample volumes in the channels are very small, a sufficiently large volume of the reservoirs will dilute the analytes so much so that they should be undetectable when they run back through the detector from the waste reservoir. Care should be taken to regularly changing the buffer in the waste reservoirs.

2.3.3 Dimension of MCE channels

The two main factors defining the microchip are the length of the separation channel and the length of the sample plug. To compare different designs, comparing the performance is necessary. Following the definitions used in chromatographic separations, the terms number of theoretical plates, plate height and resolution are used [30].

The plate number N is defined by the spatial variance of a zone σ^2 (m^2) after migrating a distance L (m):

$$N = \frac{L^2}{\sigma^2} \qquad \text{(Equation 2.12)}$$

By analogy, the plate height H (m) is given by:

$$H = \frac{L}{N} = \frac{\sigma^2}{L} \qquad \text{(Equation 2.13)}$$

Ideally, the broadening of the zone is the result of only molecular diffusion in the time interval, t (s) before the analyte zone reaches the detector. The spatial variance resulting from the diffusion of an initial infinitely small zone with a diffusion coefficient, D ($m^2 \cdot s^{-1}$) is provided by the Einstein equation:

$$\sigma^2_{diff} = 2Dt \qquad \text{(Equation 2.14)}$$

Combining equations 2.12, 2.13, and 2.14 yield the plate number under ideal conditions given below:

$$N = \frac{\mu V}{2D} \qquad \text{(Equation 2.15)}$$

This equation forms the basis of MCE. It shows that the separation efficiency is independent of the channel length as long as diffusion solely determines the spatial variance. The only experimentally accessible parameter is the applied voltage V.

The diffusion constant and electrophoretic mobility both involve movement through the medium and can be converted into one another:

$$D = \frac{\mu RT}{ZF} \qquad \text{(Equation 2.16)}$$

Equations 2.15, and 2.16 demonstrate that the plate number is also not affected by the mobility or diffusion constant since they cancel each other out.

2.3.4 Material for microchip fabrication

The first MCE used glass such as quartz, borosilicate, and soda lime, since the techniques for fabrication in these materials were well developed. These techniques are expensive, time-consuming, complicated, relatively difficult for fabrication, and require access to specialized facilities. To resolve this problem, polymer such as polyethylene terephthalate (PET), polycarbonate (PC), poly(methyl methacrylate) (PMMA), and poly(dimethylsiloxane) (PDMS) were used. The fabrication of MCE in polymers is easy; the use of polymer as materials reduces the time, complexity, and cost of prototyping and manufacturing. PDMS has been one the most actively developed polymers for MCE.

2.3.4.1 Poly(dimethylsiloxane)

Poly(dimethylsiloxane) (PDMS) have empirical formula of $(R_2SiO)_n$ and might be expected to be similar in structure and chemistry to organic ketones, a group whose empirical formular is R_2CO. These PDMS molecules were originally named silicones on the belief that they were silicon analogs of ketones. In reality, silicones have little in common with ketones. Ketones exist as discrete molecules possessing a carbon-oxygen double bond, while silicones consist of polymeric chains with an alternating silicon-oxygen backbone having with two alkyl groups bonded to each silicon atom.

PDMS are viscoelastic materials, which behave like viscous liquids at high temperature or when allowed to flow over a long period of time. They behave like elastic solids or elastomers at low temperature. This elastic behavior stems from the very flexible silicon-oxygen bonds whose angle can easily opened and closed in a scissor-like fashion. When the molecular weight is high, these flexible chains become

loosely entangled, imparting a high level of viscoelasticity. PDMS, which has the repeating $(CH_3)_2SiO$ unit, is the most common of the organosilicones. Altering the number of repeat units (value of *n*) in the chain and the degree of cross-linking which ties multiple polymer chains together generates polymers possessing different physical properties. Fluids, emulsions, lubricants, resins, elastomers or rubbers are different classes of commercially important PDMS products. Because silicon-chlorine bonds are very susceptible to cleavage by water, polydimethylsiloxane can be synthesized by hydrolyzing dichlorodimethylsilane. The initial hydrolysis reaction exothermically generates a silanol $i(CH_3)_2(OH)_2$ which readily condenses through the loss of water to form the siloxane polymer. Because dichlorodimethylsilane is bifunctional (has two chlorines), the chain is able to propagate in two directions generating high molecular weight polymers which retain some residual hydroxyl groups. These residual hydroxyl groups react with boric acid $B(OH)_3$ to form Si-O-B linkages between the polysiloxane chains. Because boric acid is trifunctional, a single boron has the ability to join three polysiloxane chains together, this joining of chains is called cross-linking. Cross-linking produces a high molecular weight polymer that is a soft, pliable gum with very interesting chemical properties [19]. Figure 2.15 shows the structure of PDMS. The physical and chemical properties of PDMS are shown in table 2.1

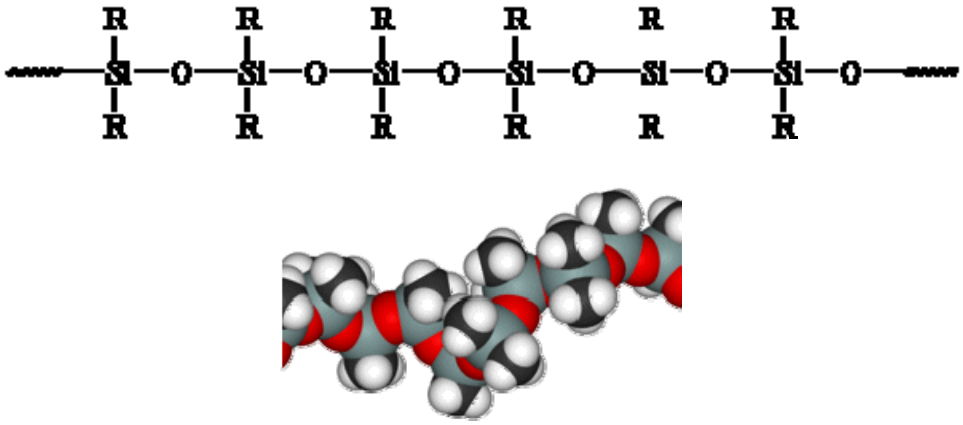

Figure 2.15 The chemical structure of PDMS [19].

Table 2.1 Physical and Chemical Properties of PDMS [53]

Property	characteristic	Consequence
Optical	transparent; UV cutoff, 240 nm	optical detection from 240 to 1100 nm
Electrical	insulating; breakdown voltage, 2×10^7 V·m^{-1}	allows embedded circuits; intentional breakdown to open connections
Mechanical	elastomeric; tunable Young's modulus, typical value of ~750 kPa	conforms to surfaces; allows actuation by reversible deformation; 24 facilitates release from molds
Thermal	insulating; thermal conductivity, 0.2 W·m^{-1}·K^{-1}; coefficient of thermal expansion, 310 μm·m^{-1}·°C^{-1}	can be used to insulate heated solutions; 64 does not allow dissipation of resistive heating from electrophoretic separation
Interfacial	low surface free energy ~20 erg·cm^2	replicas release easily from molds; can be reversibly sealed to materials
permeability	impermeable to liquid water; permeable to gases and nonpolar organic solvents	contains aqueous solutions in channels; allows gas transport through the bulk material; incompatible with many organic solvents
Reactivity	inert; can be oxidized by exposure to a plasma; $Bu_4N^+F^-$ ((TBA)F)	unreactive toward most reagents; surface can be etched; can be modified to be hydrophilic and also reactive toward silanes; etching with (TBA)F can alter topography of surfaces
Toxicity	Nontoxic.	can be implanted in vivo; supports mammalian cell growth.

2.3.5 Detection methods for MCE

MCE has been an interesting and well-studied booming research topic, demonstrating the feasibility of a chemical analysis system on a glass substrate using an electrokinetic phenomenon. However, a sensitive and miniature detection method was essential to fully exhibit the advantages of MCE. Although laser-induced fluorescence (LIF) was the most widely used detection method for its high sensitivity, the conventional LIF device was rather complicated and expensive, making the miniaturization difficult. The diode laser was small but was only available in a limited number of wavelengths. Furthermore, derivatization of the analyte with a fluorophore was often necessary. MCE coupled with mass spectrometry (MS) provided much chemical information about the analyte of intereast but was not ideal because it was inherently not portable, and costly. Chemiluminescence (CL) was a sensitive detection method especially for some metal ions. The components of CL are also simple, but accessorial devices (e.g., a pump) were needed to mix various of reagents; the susceptibility to pH as well as flow rate also weakened the merits of CL. Electrochemical detection was a good alternative given its inherent miniaturization capacity and high sensitivity. In addition, amperometric detection is the most sensitive and widely used in MCE [24,28]. In this thesis we chose amperometric detection for the detection of cholesterol.

2.4 Cholesterol

The word cholesterol comes from the Greek words “chole”, meaning “bile”, and the Greek word “stereos”, meaning “solid” or “stiff”. Cholesterol is a steroid metabolite of waxy nature, which is transported in the blood plasma of all animals. It is an essential structural component of mammalian cell membranes, where it is required to establish proper membrane permeability and fluidity. In addition, cholesterol is an important component in the manufacture of bile acids, steroid hormones, and several fat-soluble vitamins. Cholesterol is the principal sterol synthesized by animals, but small quantities are also synthesized in other eukaryotes, such as plants and fungi. It is almost completely absent

among prokaryotes, which include bacteria. The structural of cholesterol is shown in Figure 2.16

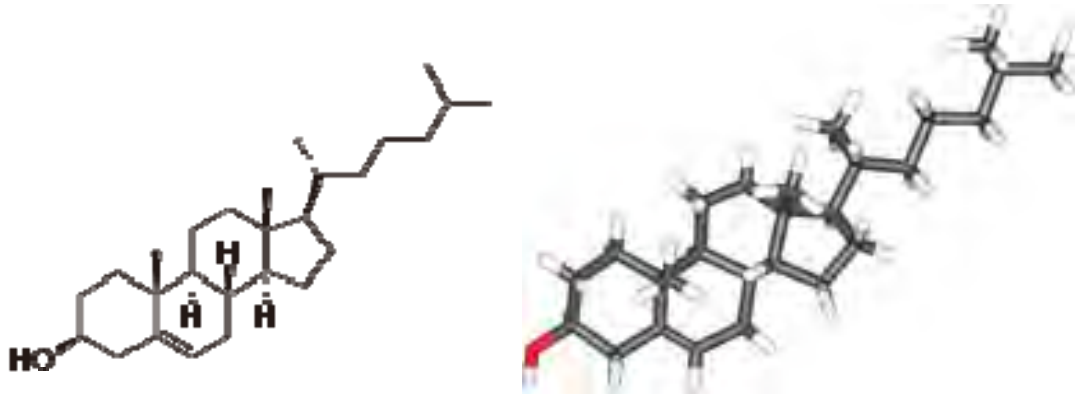

Figure 2.16 The chemical structure of cholesterol.

Cholesterol is carried in the blood by molecules called lipoproteins. A lipoprotein is any complex or compound containing both lipid (fat) and protein. The three main types are described below [54-55]:

- LDL (low density lipoprotein) – it is often referred to as bad cholesterol. LDL carries cholesterol from the liver to cells. If too much cholesterol is carried, there can be too much LDL for the cells to use, leading to harmful buildup of LDL. This lipoprotein can increase the risk of arterial disease if its levels are too high. Most human blood contains approximately 70% LDL, aithough this may vary in different persons.
- HDL (high density lipoprotein) – it is often referred to as good cholesterol. Experts say that HDL prevents arterial disease. HDL does the opposite of LDL: it takes the cholesterol away from the cells and back to the liver. In the liver HDL is either broken down or expelled from the body as waste.
- Triglycerides - these are the chemical forms in which most fat and food exist in the body. They are present in blood plasma. Triglycerides, in association with cholesterol, form the plasma lipids (blood fat). Triglycerides in plasma originate either from fats in our food or are made in the body from other energy sources, such as carbohydrates. The calories we consume that are not

immediately used by our tissues are converted into triglycerides and stored in fat cells. When the body needs energy and there is no food as an energy source, triglycerides will be released from fat cells and used; hormones control this process.

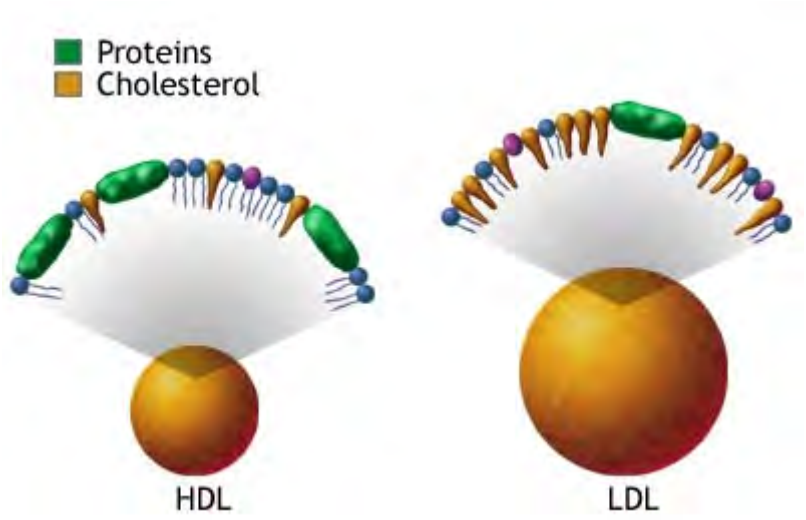

Figure 2.17 Lipoproteins vary in size and composition.

Increased blood cholesterol levels, or more specifically, increased levels of low density lipoprotein (LDL)-cholesterol, are causally related to an increased risk of coronary heart disease. Coronary risk rises progressively with an increase in cholesterol level, particularly when cholesterol levels rise above 200 $mg \cdot dL^{-1}$. The classification of cholesterol in the human blood is shown in Table 2.2. There is also substantial evidence showing that lowering total and LDL-cholesterol levels will reduce the incidence of coronary heart disease. Two approaches can be used to lower blood cholesterol levels. The first is the subject of this report: a patient-based approach that seeks to identify individuals at high risk who will benefit from intensive intervention efforts. The goal here is to establish criteria that define the candidates for medical intervention and to provide guidelines on how to detect, set goals for, treat, and monitor these patients over time. The second approach, the population (public health) strategy, aims to shift the distribution of cholesterol levels in the entire population to a lower range. These two approaches are complementary; together, they

represent a coordinated strategy aimed at reducing cholesterol levels and coronary risk.

Table 2.2 Classification of total cholesterol in the blood [2]

Level ($mg \cdot dL^{-1}$)	**Level** ($mmol \cdot L^{-1}$)	**Interpretation**
< 200	< 5.0	Desirable level corresponding to lower blood cholesterol
200 to 239	5.2 to 6.2	Borderline high blood cholesterol
> 240	> 6.2	High blood cholesterol

Along with cholesterol testing, all adults should also be evaluated for the presence of other coronary heart disease risk factors, including hypertension, smoking, Diabetes mellitus, severe obesity, and a history of coronary heart disease in the patient, or a history of premature coronary heart disease in family members. Patients with other risk factors should be given other forms of preventive care as appropriate. Patients with low blood cholesterol levels (< 200 $mg \cdot dL^{-1}$) should be given general dietary and risk reduction educational materials as well as advised to test their serum cholesterol level within five years. Patients with cholesterol levels of 200 $mg \cdot dL^{-1}$ or above should have the value confirmed by repeating the test; the average of the two test results is then used to guide subsequent decisions. Patients with high blood cholesterol (≥ 240 $mg \cdot dL^{-1}$) should undergo lipoprotein analysis, as should those with borderline-high blood cholesterol (200 to 239 $mg \cdot dL^{-1}$). These patients are at high risk because they either have coronary heart disease or other coronary heart disease risk factors.

2.5 Literature surveys

2.5.1 Biosensors

Vidal et al. (2000) developed a cholesterol amperometric biosensor that was based on a multilayer configuration, where an initial platinized layer was electrodeposited on the electrode surface and two polymer layers were sequentially electrosynthesized [9]. The hydrogen peroxide product of this biosensor was detected by amperometry.

In 2007, Arya et al. developed a biosensor for the determination of cholesterol by the immobilized ChOx-modified AEAPTS bioelectrodes were used for the estimation of cholesterol in solution using the UV–visible technique [3]. These cholesterol sensing bioelectrodes showed linearity from 50 to 500 $mg \cdot dL^{-1}$ for the cholesterol solution and a detection limit of 25 $mg \cdot dL^{-1}$.

In the same year, Dhand et al. (2007) developed a biosensor for the determination of cholesterol by the immobilization the ChOx enzyme onto electrophoretically deposited conducting polymer film (on indium-tin-oxide (ITO) glass plate) derived from a nano-structured polyaniline (PANI) colloidal suspension using *N*-ethyl-*N*'-(3-dimethyla-minopropyl) corbodiimide (EDC) and *N*-hydroxysuccinimide (NHS) chemistry [4]. The hydrogen peroxide produced of this biosensor were detected by spectrophotometry. The bioelectrodes exhibited the linearity from 25 $mg \cdot dL^{-1}$ to 400 $mg \cdot dL^{-1}$ of cholesterol, with a detection limit of 25 $mg \cdot dL^{-1}$

In 2008, Khan et al. produced the zinc oxide nanoparticles-chitosan composite film for a cholesterol biosensor [5]. Zinc oxide nanoparticles (NanoZnO) that were uniformly dispersed in chitosan (CHIT) were used to fabricate a hybrid nanocomposite film onto an indium-tin-oxide (ITO) glass plate. ChOx was immobilized onto this NanoZnO–CHIT composite film using a physisorption technique. In This case, the bioelectrodes exhibited linearity from 5 $mg \cdot dL^{-1}$ to 300 $mg \cdot dL^{-1}$of cholesterol, with a detection limit a of 5 $mg \cdot dL^{-1}$.

Unfortunately, biosensor working with the spectrophotometric technique are complicated require expensive of instrument and reagents, and experience interference from matrix species, such as ascorbic acid and uric acid.

2.5.2 Microchip capillary electrophoresis

In the past decade, microchip capillary electrophoresis has been developed for medical and biological applications. Enzyme sensor chips based on electrochemical detection have been widely studied by many researchers. However, almost all the studies focused on the fabrication of small electrodes and chambers, or on the ways to immobilize the enzyme on the surface of the electrode and on chips.

In 2000, Wang et al. developed glass microchip capillary electrophoresis for the detection of glucose, uric acid, ascorbic acid, and acetaminophen by amperometric detection [11]. The enzymatically liberated neutral peroxide species was separated electrophoretically from the anionic uric and ascorbic acids in the separation/reaction channel. The three oxidizable species were detected at the downstream gold-coated thickfilm amperometric detector at different migration times.

In 2003, Wang et al developed glass microchip capillary electrophoresis for the detection of renal markers creatine, creatinine, *p*-aminohippuric acid, and uric acid by amperometric detection [12]. The peroxide product as well as the oxidizable *p*-aminohippuric and uric acids were detected electrochemically at a downstream gold-coated thick-film amperometric detector. The four renal markers are readily measured (within 5 min), while creatinine/creatine was detected in less than 2 min.

In 2003, Carlos et al. used a PDMS polymer microchip for the detection of underivatized carbohydrates, amino acids, and sulfur-containing antibiotics in an electrophoretic microchip using pulsed amperometric detection (PAD) [29]. The advantage of PDMS was its ability to generate a tight seal to itself or other flat surfaces, reversibly or irreversibly, without the distortion of the micro-channels. The detection limits ranged from 6 fmol (5 μM) for penicillin and ampicillin, to 455 fmol (350 μM) for histidine.

In 2004, Lee et al. developed the microchip capillary electrophoresis fabricated from glass using platinum as a working electrode coupled with an

electrochemical detector for the precolumn enzymatic analysis of glucose, creatinine, uric acid and ascorbic acid in urine and serum [13]. The detection limits (S/N = 3) ranged from 0.71 μM for ascorbic acid and glucose, to 10 μM. The calibration curve was linear from 10 μM to 800 μM (R^2 > 0.995).

In 2005, Ping et al. reported a method for the rapid analysis of lipoproteins by microchip electrophoresis with light-emitting diode confocal fluorescence detection [22]. Lipoproteins labeled with BODIPY FL C5-ceramide are found to strongly adsorb on the bare surface of a poly(methylmetha-crylate) (PMMA) microchip. Sodium dodecyl sulfate and cetyltrimethylammonium bromide were therefore utilized to alter lipoproteins and a channel surface to make them bear the same type of charge. After this modification, the peak shape of lipoproteins was greatly improved, demonstrating that lipoprotein adsorption on a PMMA chip was dramatically reduced due to electrostatic repulsion. In addition, polymers were added into the running buffer to suppress electroosmotic flow and to serve as a sieving matrix.

In this thesis, the PDMS microchip coupled with enzymatic assay and amperometric detection is a promising alternative method for the detection of cholesterol over because it is easy to use, requires small volumes of reagents and sample, and provide rapid analysis. The hydrogen peroxide product is detected with amperometric detection at the gold wire working electrode.

CHAPTER III

EXPERIMENTAL

This chapter has provided the information of chemical and reagents, instruments and equipments and sample preparation.

3.1 Chemical and reagents

3.1.1 Sylgard 184 silicone elastomer and curing agent (Dow Corning, Midland, MI, USA)

3.1.2 Cholesterol ≥ 99 % (Sigma, St. Louis, MO)

3.1.3 Cholesterol oxidase from *Streptomyces* sp. (Sigma, St. Louis, MO)

3.1.4 2-Morpholinoethanesulfonic acid monohydrate (MES) (Sigma, St. Louis, MO)

3.1.5 Dopamine hydrochloride (Sigma, St. Louis, MO)

3.1.6 Pyrocatechol (Fluka, Switzerland)

3.1.7 Potassium dihydrogen phosphate (Merk, Germany)

3.1.8 Dipotassium hydrogen phosphate (Merk, Germany)

3.1.9 Lipid cholesterol rich from adult bovine serum (Sigma, St. Louis, MO)

3.1.10 Methanol (Merk, Germany)

3.1.11 Sodium hydroxide (Merk, Germany)

3.1.12 Hydrochloric acid (Merk, Germany)

3.1.13 L(+)-Ascorbic acid (Wako Pure Chemical Industries, Ltd, Japan)

3.1.14 Triton X-100 for molecular biology (Sigma, St. Louis, MO)

3.1.15 Gold (Au) 99.99%, diameter 25 μm (Goodfellow, England)

3.1.16 Platinum 99.99%, diameter 50 μm (Goodfellow, England)

3.1.17 Silicon wafer (UniversityWafer, South Boston, MA)

3.1.18 SU-8 3025 (Microchem, Newton, MA)

3.1.19 SU-8 Developer (Microchem, Newton, MA)

3.1.20 2-Propanol (Merk, Germany)

3.1.21 Acetone (Merk, Germany)

3.2 Instruments and equipments

3.2.1 CHI1232a (CH-instrument,USA)
3.2.2 Analytical balance (Mettler AT 200, Mettler, Swizerland)
3.2.3 pH meter (Metrohm 744 pH meter, Metrohm, Switzerland)
3.2.4 Homemade high-voltage power supply
3.2.5 Air plasma cleaner (PDG-32G, Harrick plasma
3.2.6 Microscope (SZ-PT, Olympus, Japan)
3.2.7 Auto pipette and tips (Eppendrof, Germany)
3.2.8 G3P-8 Spincoat series from Specialty Coating Systems (USA)
3.2.9 Milli Q Water System (Millipore, USA, R ≥ 18.2 MΩ.cm)
3.2.10 Hot plate stirrer C-MAG HS 10 (IKA, Germany)
3.2.11 Vacuum Pump (Gast, USA)
3.2.12 Magnetic stirring bars (SCS ICS, Switzerland)
3.2.13 Dedicator (CSN, Simax, USA)
3.2.14 Beaker 10, 25, 50 mL
3.2.15 Volumetric flask 10, 100, 250 mL

3.3 Preparation of solutions

All standard and sample solutions were prepared by using deionized water from Milli Q Water System (Millipore, USA, R ≥ 18.2 MΩ.cm).

3.3.1 Preparation of 20 mM MES buffer, pH 7.0

MES (1.066 g) was dissolved in deionized water. The resulting solution was adjusted to the required pH with either 0.1 M sodium hydroxide or 0.1 M phosphoric acid, and diluted to 250 mL total volume with water in volumetric flask

3.3.2 Preparation of 40 mM phosphate buffer (PB buffer), pH 7.0

1.36 g potassium dihydrogen orthrophosphate was dissolved in 250 mL deionized water as a stock solution 1 and 1.74 g of dipotassium hydrogen orthrophosphate was dissolved in 250 mL deionized water as a stock solution 2. The stock solution 1 was adjusted to pH 7.0 with stock solution 2.

3.3.3 Preparation of stock standard solution of dopamine

10 mM dopamine standard solution was prepared by dissolving dopamine hydrochloride (0.0190 g) in 10 mL of 0.1 M hydrochloric acid.

3.3.4 Preparation of stock standard solution of catechol

10 mM catechol standard solution was prepared by dissolving pyrocatechol (0.0110 g) in 10 mL of 0.1 M hydrochloric acid.

3.3.5 Preparation of stock standard solution of hydrogen peroxide

100 mM hydrogen peroxide was prepared by pipette hydrogen peroxide standard solution 15 µL in 1,485 µL of deionized water.

3.3.6 Preparation of stock standard solution of ascorbic acid

10 mM ascorbic acid was prepared by dissolving ascorbic acid (0.0088 g) in 5 mL deionized water

3.3.7 Preparation of stock standard solution of cholesterol

Stock solution of 100 mM cholesterol was prepared by dissolving 3.9 mg of cholesterol in 5 % Triton X-100. The solution was gently stirred with constant speed to obtain a clear solution. After that, solution was made up to 1.00 mL by deionized water and stored at 4°C. This stock solution was further diluted to make the different concentrations of the cholesterol in deionized water and filtered with 0.45 µm filters.

3.3.8 Preparation of stock standard solution of cholesterol oxidase enzyme (39 Unit/mL)

Stock solution of ChOx was prepared by dissolving 1.0 mg of cholesterol oxidase (ChOx) in 1 mL of 40 mM phosphate buffer (PB, pH 7.0). Stock solution of ChOx was further diluted to make different concentrations in 40 mM PB buffer (pH 7.0), prior to be used.

3.4 Apparatus of PDMS microchip capillary electrophoresis

The details of microchip capillary electrophoresis were described. The microchip consisted of two crossed channels and four reservoirs, including a four-way injection cross (connected to the three reservoirs). The microchip had the channel with the wide and depth of 50 µm and the length of separation channel was 50 mm. The electrode channels were 50 µm wide and 50 µm dept. Schematic of the microchip capillary electrophoresis is shown in Figure 3.1.

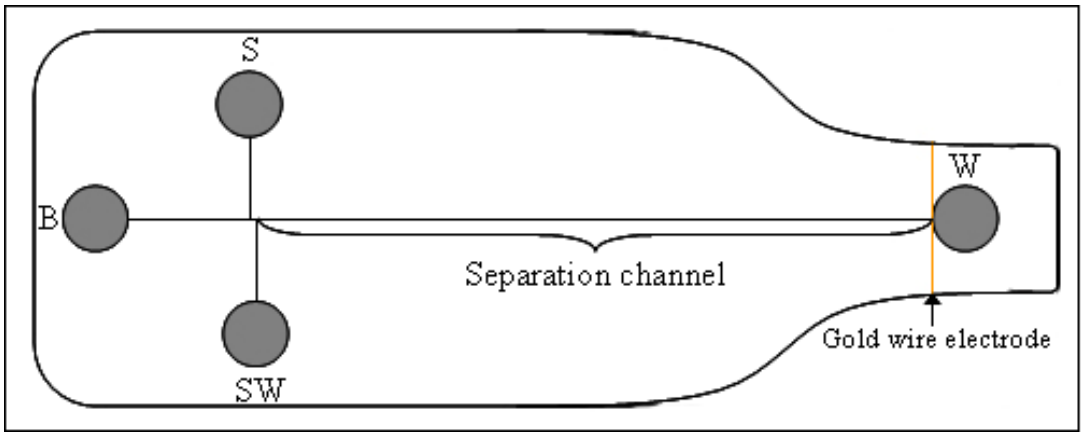

Figure 3.1 Schematic of PDMS microfluidic device. Channels: 50 μm width, 50 μm depth. 50 mm length of separation channel and 25 μm Au wire working electrode (B = PB buffer + ChOx, S = sample, SW = sample waste, and W = PB buffer).

3.5 Microchip capillary electrophoresis fabrication

3.5.1 Fabrication of a mold

The silicon wafer was cleaned with piranha solution and coated with SU-8 3025 negative photoresist using a spin coater to thickness of 50 μm. A digitally produced mask containing the channel pattern was placed on the coated wafer. The coated wafer was placed on hot plate at 65°C for 2 minute, next move to hot plate that set the temperature at 95°C for 5 min. Then, the coated wafer was exposed to light via a near-UV flood source for 7 s. After that, the coated wafer was placed on hot plate at 65°C for 3 minute, next move to hot plate that set the temperature at 95°C for 6 min. Next, the coated wafer was immersed in the developer for 5 minute and rinsed with isopropanol for 1 minute. Finally, the wafer was placed in the oven at 65°C for 30 minute.

3.5.2 Fabrication of PDMS microchip capillary electrophoresis

The fabrication of the PDMS microchip capillary electrophoresis is briefly explained. PDMS was mixed with curing agent in the ratio of 10:1 (w/w) to form a

PDMS mixture and degassed under vacuum until bubbles were all out. The PDMS mixture was poured over a molding master and a blank wafer, and cured for at least 2 h at 65 °C in the oven. After that, the cross-linked PDMS was peeled off the mold, the reservoirs were created by a circular punch and a 25 µm gold wire working electrode was placed in the electrode channel at the end of separation channel. Next, the PDMS layers were placed in an air plasma cleaner, oxidized for 60 s, and immediately brought to form an irreversible seal with a second piece of cross-linked. The end-point of the electrode channel was sealed with silicone glue. Finally, an electrical connection was made using silver paint and silver wire. The Electrical connections made from platinum electrodes were placed into reservoirs [26,29,31]. The potential at separation step and injection step were applied to the reservoir as shown in Table 3.1.

Table 3.1 Potentials applied and solution in each reservoirs on the PDMS microchip during either the injection or the separation step

Reservoir	Containing	Separation (V)	Injection (V)
B	PB buffer+ChOx	+1600	+450
S	Sample	+450	+450
SW	PB buffer	+450	–160
G	PB buffer	Ground	ground

3.6 Procedures of PDMS microchip capillary electrophoresis

3.6.1 PDMS microchip capillary electrophoresis with amperometric detection

3.6.1.1 PDMS microchip capillary electrophoresis layout

The PDMS microchip capillary electrophoresis system used in this work consisted of PDMS microchip, microfluidic system, a high voltage power supply and an electrochemical detector as shown in Figure 3.2. The PDMS microchip was placed

in copper box. The gold wire at the end of separation channel is a working electrode. Platinum wire in the microfluidic system inserted into detection reservoir served as a counter and reference electrodes.

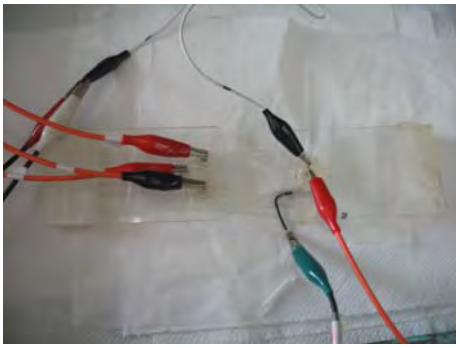

a) Microfluidic System

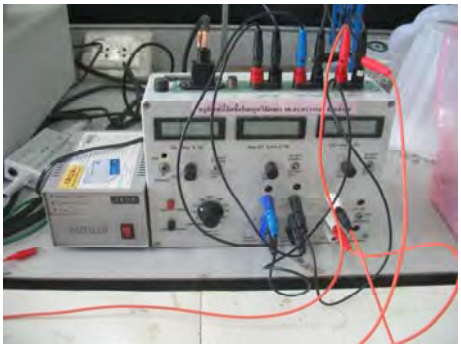

b) High Voltage Power Supply

c) Electrochemical Detection System

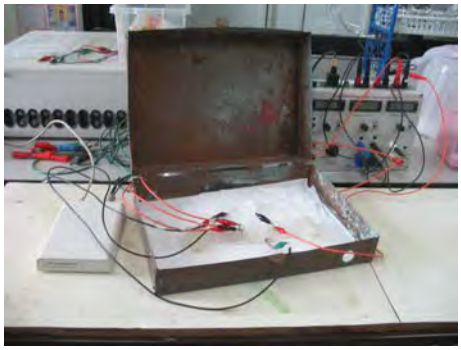

d) Full System

Figure 3.2 The PDMS microchip capillary electrophoresis with microfluidic system, a high voltage power supply and an electrochemical detection system.

3.6.1.2 Electrophoresis procedure

Prior to use, the channels were treated by rinsing with 0.1 M sodium hydroxide and deionized water for 20 and 5 min, respectively. This treatment changed a silanol groups (Si-OH) to negative form on the surface of the PDMS microchip. To perform the electrophoretic separation, waste reservoir was filled with the phosphate buffer solution, while the buffer reservoir was filled with phosphate buffer containing the cholesterol oxidase enzyme. The sample reservoir was also filled with cholesterol. For injection step, the sample and buffer reservoirs were held

at +450 V while the sample waste reservoir was held at −160 V for loading the sample plug into the double-T injector. Separation was performed by switching the high voltage contacts and applying the corresponding separation voltages to the running buffer reservoir with the detection reservoir grounded, all other reservoirs floating. Subsequent, the separation step, the separation voltage was varies from +1100 to +1600 V to the buffer reservoir. Cholesterol in separation channel was reacted with the Cholesterol oxidase enzyme in the running buffer to generate hydrogen peroxide. Finally, hydrogen peroxide was detected at the downstream gold wire electrode by amperometric detection.

3.6.1.3 Electrochemical detection

Amperometry is a one technique of electrochemical detection and it is popular to be detection for microchip capillary electrophoresis. Amperometric detection was performed with an electrochemical analyzer (CHI1232a, CH-instrument, USA) using the “amperometric i-t curve” mode. The electropherograms were recorded with a time resolution of 0.2 s while applying a desired detection potential versus platinum wire. Sample injections step were performed after stabilization of the baseline. Amperometry was used to detect a mixed standard of dopamine and catechol for the characterized of PDMS microchip and detect the cholesterol. For characterization of PDMS microchip, the constant detection potential of +0.8 V was applied to the working electrode.

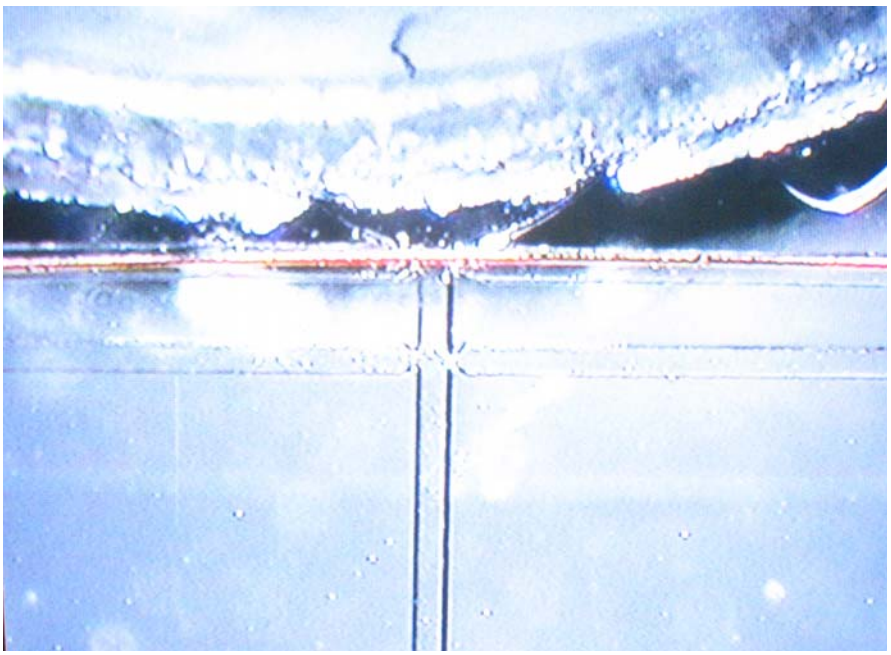

Figure 3.3 A photograph showing electrode alignment in a completed microchip.

3.6.1.4 Safety considerations

The high voltage power supply and associated open electrical connections should be handled with extremely care to prevent electrical shock. The stock solutions must be stored in closed small containers and isolated from any reducing reagents.

3.6.1.5 Detection potential dependence

These studies were done under the optimum condition of previous experiment (section 3.6.1.5-3.6.1.6) then changing the detection potential of working electrode over +0.2 V to +0.9 V.

3.6.1.6 Buffer pH dependence

The pH of buffer electrolyte was carried out by injecting flow concentration of analyte solutions under the various pH from 6 to 8 of buffer electrolyte. These experiments were done to obtain the optimum pH of buffer electrolyte for separation of the analytes. The higher the current signal and lower the migration time are the better the sensitivity and separation efficiency was obtained. Therefore, the current signal and migration time were used to indicate the optimum pH of buffer electrolyte for analysis system.

3.6.1.7 Buffer concentration dependence

The concentration of buffer electrolyte was carried out by injecting flow concentration of analyte solutions under the optimum pH of buffer electrolyte from the previous experiment (section 3.6.1.5) using various concentration from 5 mM to 50 mM of buffer electrolyte. These experiments were done to obtain

the optimum concentration of buffer electrolyte for separation of the analytes. The optimum concentration of buffer electrolyte for analysis system is obtained similar to the optimum pH of buffer electrolyte.

3.6.1.8 Cholesterol oxidase enzyme concentration dependence

The concentration of cholesterol oxidase enzyme was carried out by injecting flow concentration of analyte solutions under the optimum condition of previous experiment (section 3.6.1.5-3.6.1.7) using various concentration from 0.03 $U.mL^{-1}$ to 1.02 $U.mL^{-1}$. These experiments were done to obtain the optimum concentration of cholesterol oxidase enzyme for the determination of analytes.

3.6.1.9 Separation voltage dependence

These studies were done under the optimum condition of previous experiments (section 3.6.1.5-3.6.1.8) then varied the separation voltages from +1100 V to +1800

V. The optimum separation voltage for analysis system is obtained similar to the optimum pH of buffer electrolyte.

3.6.1.10 Injection time dependence

These studies were done the optimum condition of previous experiment in a section of 3.6.1.5 to 3.6.1.9. The injection time were varied from 5 s to 25 s. The optimum of injection time was defined the highest response.

3.6.1.11 The calibration curve and linear range

10 mM stock solution of each analyte was freshly prepared and then diluted to the range of 1 nM to 10 mM. The experiments were carried out by injection of three replicates of each concentration. The results were used to plot the calibration curve and obtain the linear range.

3.6.1.12 Limit of detection (LOD)

The limit of detection (LOD) was carried out by injecting the each concentration of analyte solutions for three replicates. The limit of detection was defined as the concentration that provided a current response three time higher than noise ($S/N \geq 3$)

3.6.1.13 Limit of quantitation (LOQ)

The limit of quantitation (LOQ) was carried out by injecting the each concentration of analyte solutions for three replicates. The limit of quantitation was defined as the concentration that provided a current response three times higher than noise ($S/N \geq 10$)

3.6.1.14 Repeatability

The repeatability was studied by injecting ten replicates of analyte solution. The repeatability is assessed in term of the relative standard deviation (%RSD), using the following formula:

$$\%RSD = \frac{\text{Standard deviation}}{\text{Mean}} \times 100$$

3.6.2 Applications

3.6.2.1 Serum sample analysis

A serum sample solution from adult bovine serum was prepared by dissolving 75 mg of serum in 1.0 mL of 40 mM phosphate buffer (PB, pH 7.0). A serum sample solution were spiked with cholesterol stock solution and further diluted with 40 mM PB buffer pH 7.0 to obtain various concentrations. Finally, the solutions were analyted by PDMS microchip capillary electrophoresis.

CHAPTER IV

RESULTS AND DISCUSSION

This chapter focused on the results obtained from the development of PDMS microchip capillary electrophoresis coupled with electrochemical detection for the determination of cholesterol. In the following sections, the optimization of factors influencing the performance, such as the concentration of running buffer, pH of running buffer, concentration of enzyme cholesterol oxidase, separation voltage, injection time and detection potential is described. Finally, the determination of cholesterol in serum was measured by PDMS microchip capillary electrophoresis.

4.1 Characterization of PDMS microchip capillary electrophoresis

Amperometric detection was used during the characterization of PDMS microchip capillary electrophoresis. The standards dopamine and catechol were chosen as analytes to evaluate the performance of PDMS microchip capillary electrophoresis.

The PDMS microfluidic device was characterized by the separation and detection of a mixed standard of 250 μM dopamine and 250 μM catechol. MES buffer (20 mM, pH 7.0) was used as a running buffer, the separation voltage was set at +1300 V with an injection time of 20 s. A detection potential of +0.8 V was selected as optimal; a typical electropherogram is depicted in Figure 4.1. It can be observed that the mixed standard was well separated by the prepared PDMS microchip. This result indicated that the prepared PDMS microchip was suitable for the separation of the other compounds.

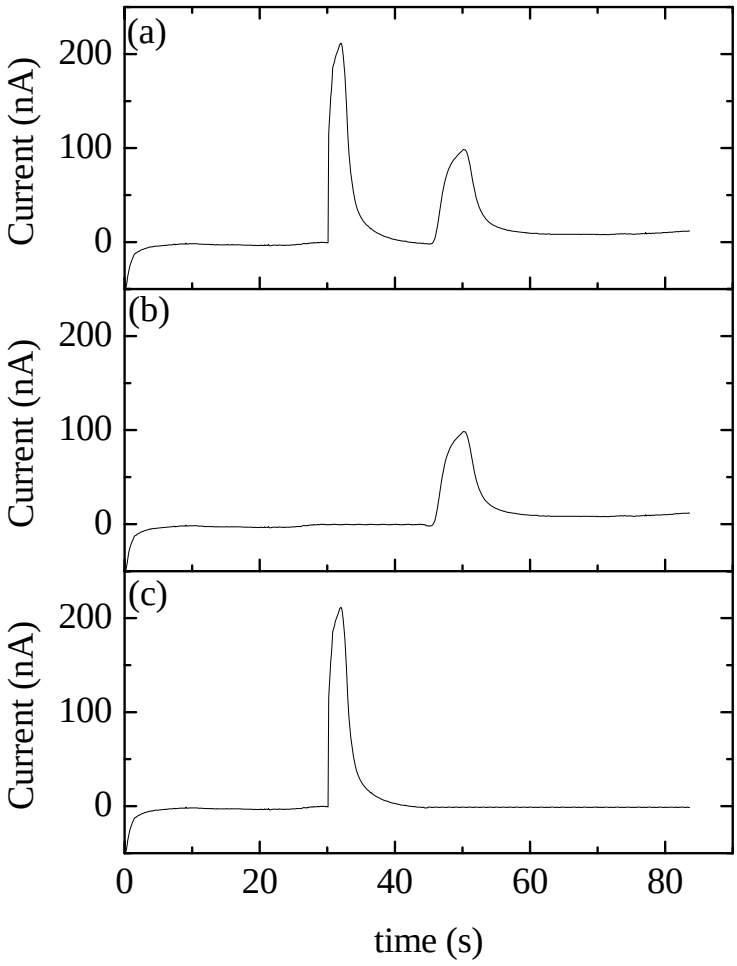

Figure 4.1 The characterization of PDMS Microchip capillary electrophoresis (a) Electropherogram of mixed 250 µM dopamine and 250 µM catechol, (b) and (c) is 250 µM dopamine and 250 µM catechol, respectively. Conditions: running buffer, a MES buffer (20 mM, pH 7.0) solution; separation potential, +1300 V; injection potential, +450 V; injection time, 20 s; detection potential, +0.8 V at 25 µm Au wire working electrode.

4.2 PDMS Microchip capillary electrophoresis for the quantification of cholesterol levels

As mentioned previously, the ultimate goal of this work was to develop miniaturized clinical analyzers by coupling enzymatic assays in the PDMS microchips channel, the ChOx enzyme prepared in running buffer and sample solutions were mixed at the channel intersection and in the separation channel using electrokinetic flow. The enzymatic reaction occurred along the separation/reaction channel. Schematic 1 showed the enzyme reaction and the detection at the electrode surface.

Separation channel:

$$\text{Cholesterol} + O_2 \xrightarrow{\text{ChOx}} \text{cholestenone} + HOOH$$

Electrode:

$$HOOH + 2H^+ + 2e^- \longrightarrow 2H_2O$$

Schematic 1. The enzymatic reaction of cholesterol in the separation channel and detection electrode.

4.2.1 Effect of detection potential

The detection potential strongly affects to the sensitivity of the PDMS microchip capillary electrophoresis system in the electrochemical mode. To obtain the optimal detection potential, a hydrodynamic voltammogram was constructed as shown in Figure 4.2.

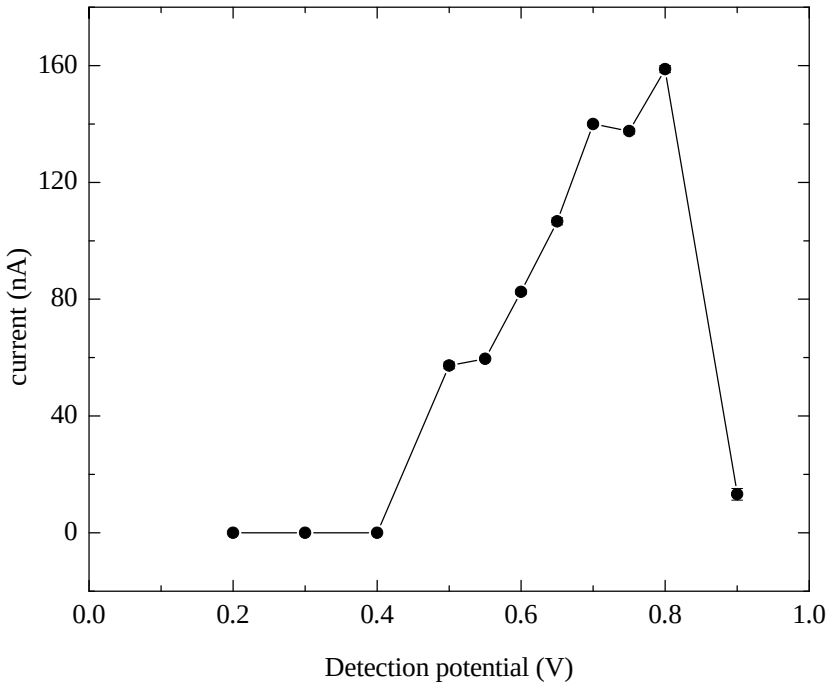

Figure 4.2 Hydrodynamic voltammogram of 1.0 mM hydrogen peroxide. Conditions: running buffer, a PB buffer (10 mM, pH 7.0) solution; separation potential, +1300 V; injection potential, +450 V; injection time, 20 s; at 25 μm Au wire working electrode.

A hydrodynamic voltammogram for hydrogen peroxide detection was obtained by changing the detection potential on the gold wire working electrode over the range of +0.2 V to +0.9 V. The height of the peak current rapidly increased from +0.4 V to +0.8 V and then leveled off. Therefore, +0.5 V was chosen as the optimal detection potential because any higher detection potentials would likely increase the interference effect from ascorbic acid in serum samples.

4.2.2 Effect of running buffer concentration

The concentrations of running buffer is an important parameter, which affects the sensitivity of the peak current and the separation efficiency of cholesterol. An electropherogram at 1 mM cholesterol was performed. The concentration of running buffer was studied over the concentration range of 5 mM to 50 mM. The effect of concentration on the peak current of cholesterol is illustrated in Figure 4.3. The peak current of 1 mM cholesterol was found to increased when the concentration of

running buffer increased from 5 mM to 40 mM; and the peak current then decreased with any further increase in the concentration of running buffer. This phenomenon may be of concern given that the higher concentration of running buffer will increase the ionic strength. With regard to sensitivity of the peak current, the concentration of running buffer at 40 mM was selected for the determination of cholesterol.

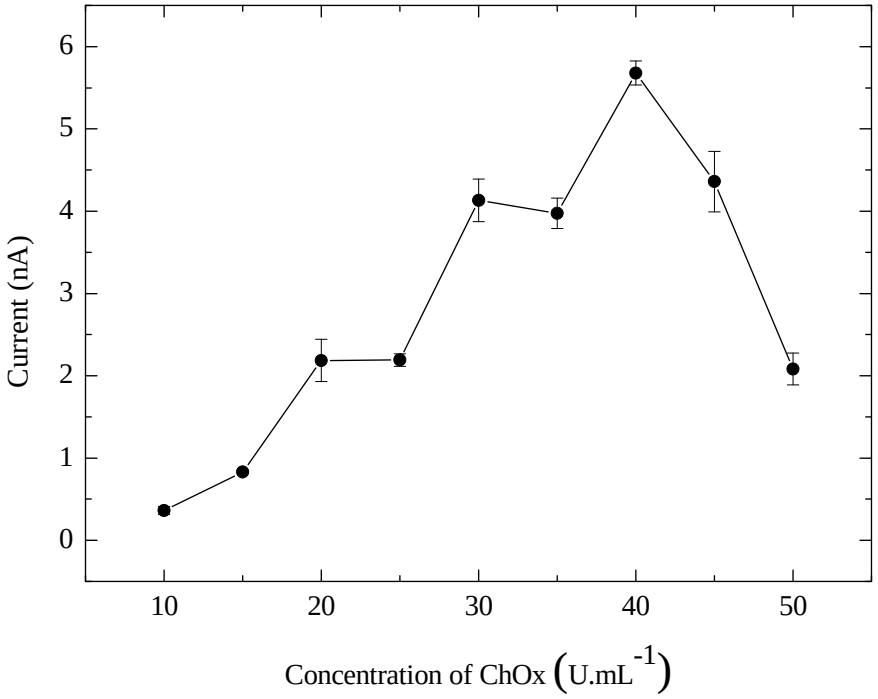

Figure 4.3 The effect of running buffer concentration on peak current of -1 mM cholesterol. Conditions: running buffer, a PB buffer (pH 7.0) solution; detection potential, +0.5 V, separation potential, +1300 V; injection potential, +450 V; injection time, 20 s; at 25 µm Au wire working electrode.

4.2.3 Effect of running buffer pH

The running buffer pH affects the EOF velocity, enzyme activity, migration time, and separation efficiency of the analyte. Hence, the optimal pH values were determined by varying the pH of the running buffer from 6.0 to 8.0 as shown in Figures 4.4 and 4.5. First, the effect of the running buffer pH on the migration time

and enzyme activity on peak current was monitored. It was found that the migration time of 1 mM cholesterol decreased when the running buffer pH increased from 6.0 to 7.0 and then increased with a further increase of the running buffer until 7.2 after that the migration time seem to be constant. Second, the effect of the running buffer pH on peak current and ChOx enzyme activity was decribed. Then, the peak current increased until 7.0 after that the peak current became constant. In addition the enzyme activity decreased in more acid or basic conditions. Interestingly, the minimum of migration time with maximum ChOx enzyme activity was obtained at pH 7.0. Thus, a running buffer at pH 7.0 was used in all experiments.

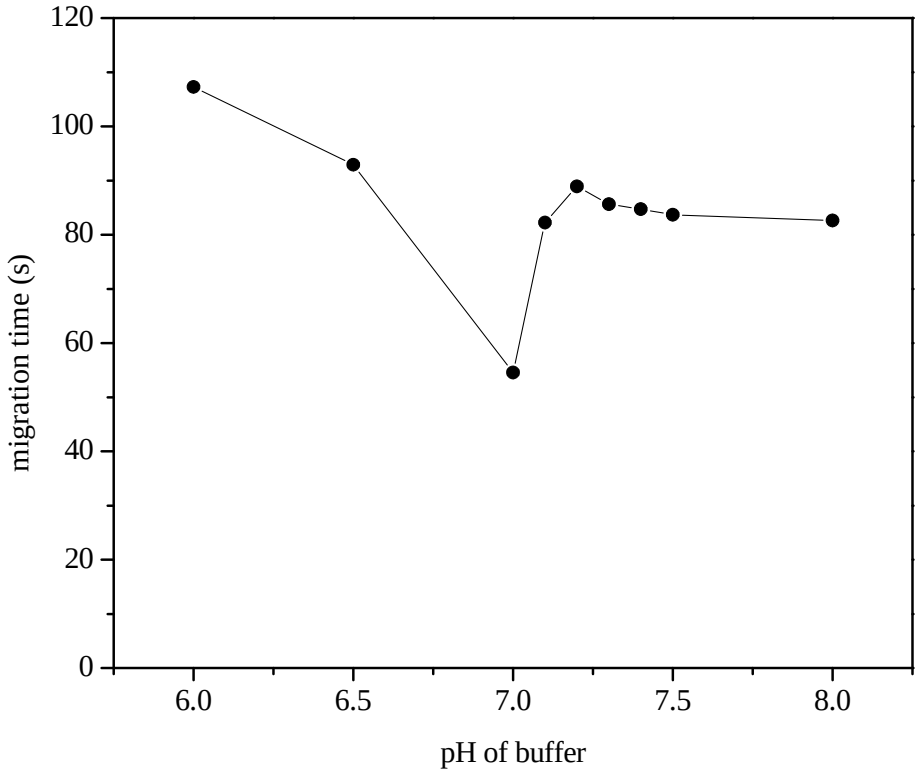

Figure 4.4 The effect of running buffer pH on migration time of 0.1 mM Cholesterol. Conditions: running buffer, a PB buffer (40 mM, pH 7.0) solution containing 0.034 $U \cdot mL^{-1}$; detection potential, +0.5 V, separation potential, +1300 V; injection potential, +450 V; injection time, 20 s; at 25 μm Au wire working electrode.

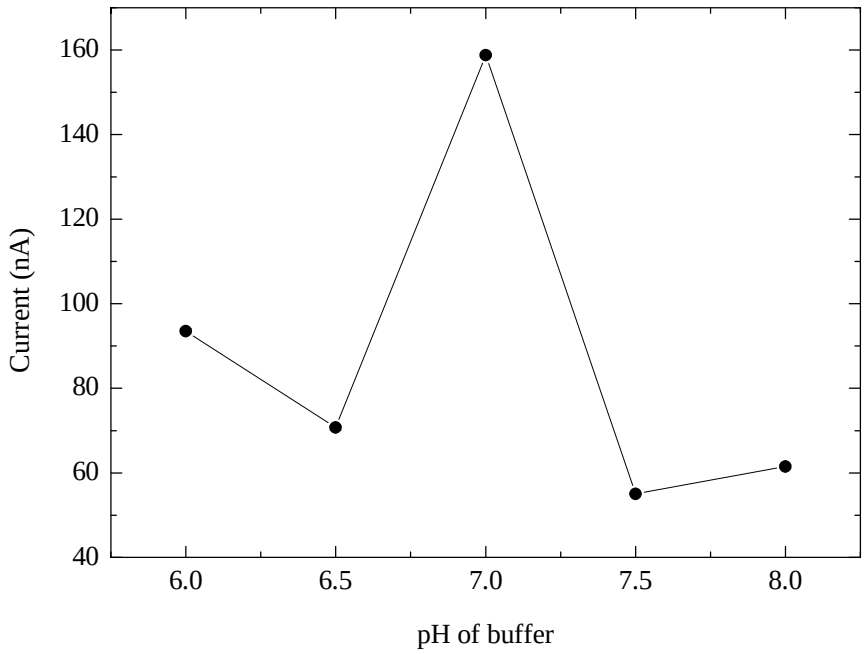

Figure 4.5 The effect of running buffer pH on peak current of 0.1 mM Cholesterol. Conditions: running buffer, a PB buffer (40 mM, pH 7.0) solution containing 0.034 $U \cdot mL^{-1}$; detection potential, +0.5 V, separation potential, +1300 V; injection potential, +450 V; time, 20 s; at 25 µm Au wire working electrode.

4.2.4 Effect of solvent on the cholesterol solubility

Water, 10 mM PB and running buffer were used as cholesterol solvents. The peak current of 1 mM of cholesterol dissolved in water, 10 mM PB buffer, and running buffer is shown in Figure 4.6. The peak current of 1 mM cholesterol was increased when using water as the solvent because the sample becomes more concentrated inside the channel, and peak efficiency is increasing by sample stacking. Sample stacking occurred when the sample was dissolved in a lower ionic strength solution than in separation electrolyte. The effect of cholesterol solvent on the peak current is illustrated in Figure 4.6. The highest current was observed when water was used as the solvent. Therefore, water was chosen as solvent to dissolve the cholesterol standard before injection into the channel.

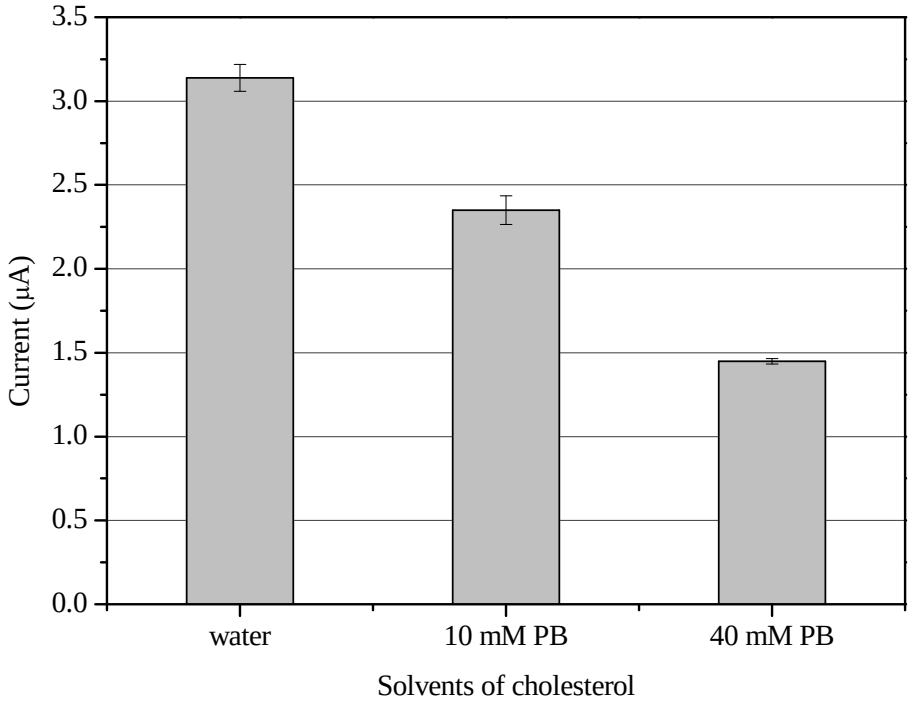

Figure 4.6 The effect of solvent on peak current of 1 mM Cholesterol. Conditions: running buffer, a PB buffer (40 mM, pH 7.0) solution containing 0.034 $U \cdot mL^{-1}$; detection potential, +0.5 V, separation potential, +1300 V; injection potential, +450 V; injection time, 20 s; at 25 μm Au wire working electrode.

4.2.5 Effect of cholesterol oxidase enzyme concentration

The concentration of the cholesterol oxidase enzyme (ChOx) also affected to the peak current of cholesterol because the enzyme can convert cholesterol to hydrogen peroxide. Figure 4.7 dispalys the effect of ChOx concentration in the reagent solution in the response to the 1 mM cholesterol substrate. The current rapidly increased when the ChOx concentration was increased from 0.034 $U \cdot mL^{-1}$ to 0.68 $U \cdot mL^{-1}$, and finally leveled off above enzyme concentration of the 0.85 $U \cdot mL^{-1}$; the high concentrations of enzyme resulted in increased background noise and adsorption onto the channel walls. The optimal response was obtained at 0.68 $U \cdot mL^{-1}$.

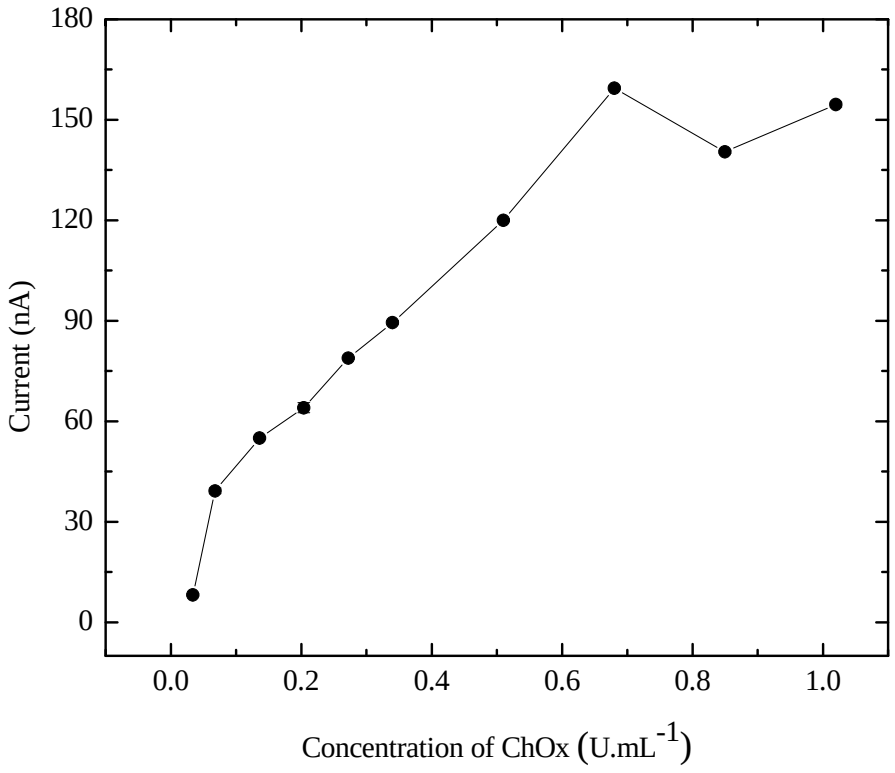

Figure 4.7 The effect of the enzyme cholesterol oxidase containing in PB buffer (40 mM, pH 7.0) on peak current of 1 mM Cholesterol. Conditions: detection potential, +0.5 V, separation potential, +1300 V; injection potential, +450 V; inject time, 20 s; at 25 µm Au wire working electrode.

4.2.6 Effect of separation voltage

The separation voltage is one of the parameters that affected the electric field strength, which in turn affected the EOF and the migration time of analytes. Moreover, a higher separation voltage resulted in increased Joule heating. The relationship between the migration times of 1 mM cholesterol with different separation voltages is shown in Figures 4.8 and Figure 4.9.

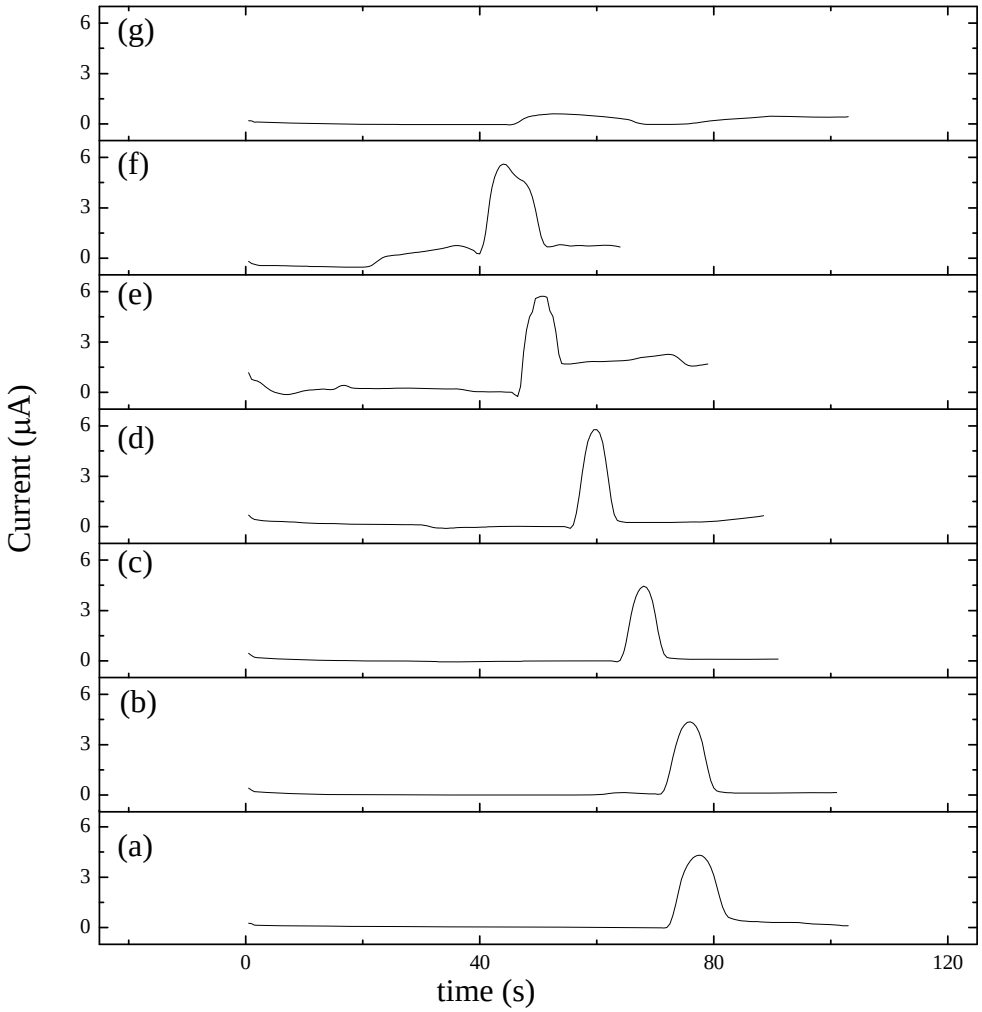

Figure 4.8 The effect of separation voltage for PDMS Microchip capillary electrophoresis. The electropherogram of 1 mM of cholesterol at different the injection time, (a) +1300 V, (b) +1400 V, (c) +1500 V, (d) +1600 V, (e) +1700 V, (f) +1800 V, and (g) +1900 V. Conditions: running buffer, a PB buffer (pH 7.0) solution containing 0.68 $U \cdot mL^{-1}$; detection potential, +0.5 V; injection potential, +450 V; injection time, 20 s; at 25 μm Au wire working electrode.

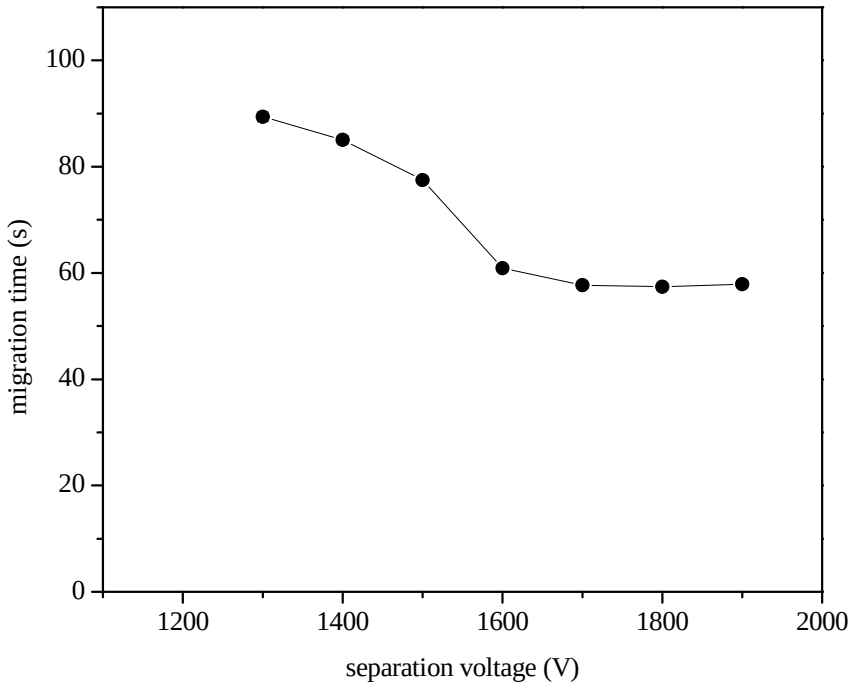

Figure 4.9 The effect of separation voltage on the peak current of 1 mM Cholesterol. Conditions: running buffer, a PB buffer (40 mM, pH 7.0) solution containing 0.68 $U \cdot mL^{-1}$; detection potential, +0.5 V; injection potential, +450 V; injection time, 20 s; at 25 μm Au wire working electrode.

The separation voltage was studied in the range of +1300 V to +1900 V. It was observed that the migration time decreased with increasing separation voltage but the baseline noise also increased. This yielded an increase in the detection limit of the analytes as well. Figure 4.9 shows that the migration time decreases rapidly upon increasing the separation voltage from +1300 V and +1600 V; after that the migration time became constant. The optimal separation voltage was +1600 V.

4.2.7 Effect of injection time

In addition to optimizing the previously mentioned condition, the length of time required for sample injection was studied. Typically, the injection time was used to control the volume of sample plug, which also greatly affected the separation

efficiency. The effect of injection time was varied from 5 s to 25 s as shown in Figure 4.10 and 4.11. As expected, the peak currents increased when injection time increased from 5 s to 20 s. However, when the time was above 20 s, peak currents became constant but the background noise was increased, leading broadening peaks. Therefore, 20 s was chosen as the suitable injection time for detection of cholesterol.

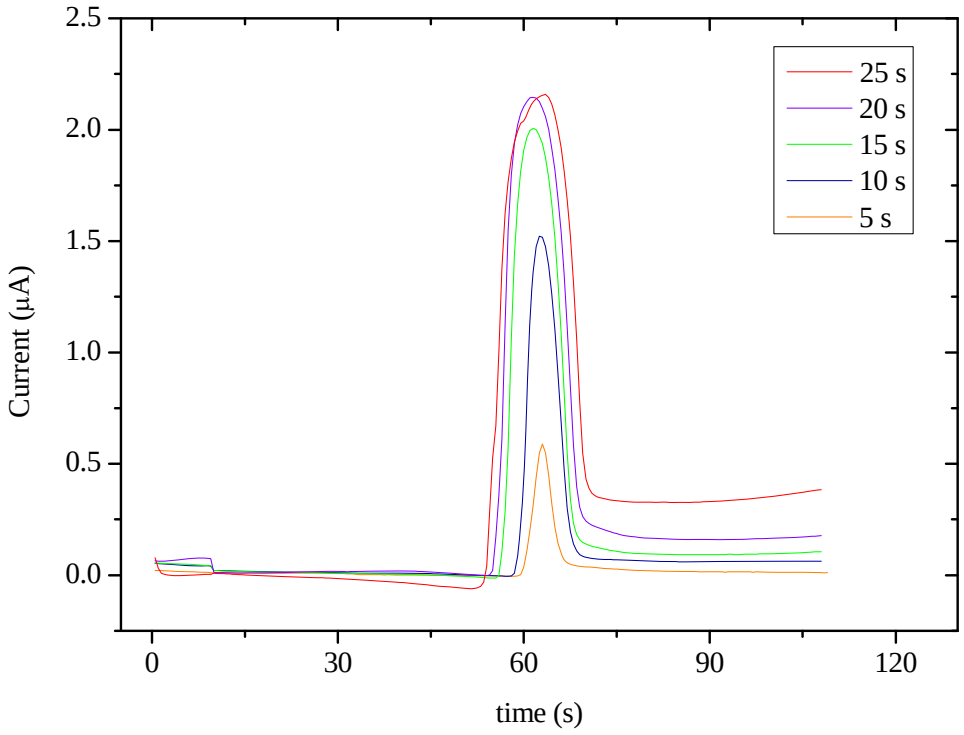

Figure 4.10 The effect of injection time for PDMS Microchip capillary electrophoresis. The electropherogram of 1 mM of cholesterol at different the injection time, (a) 5 s, (b) 10 s, (c) 15 s, (d) 20 s, and (e) 25 s. Conditions: running buffer, a PB buffer (pH 7.0) solution containing 0.68 $U \cdot mL^{-1}$; detection potential, +0.5 V, separation potential, +1600 V; injection potential, +450 V; at 25 μm Au wire working electrode.

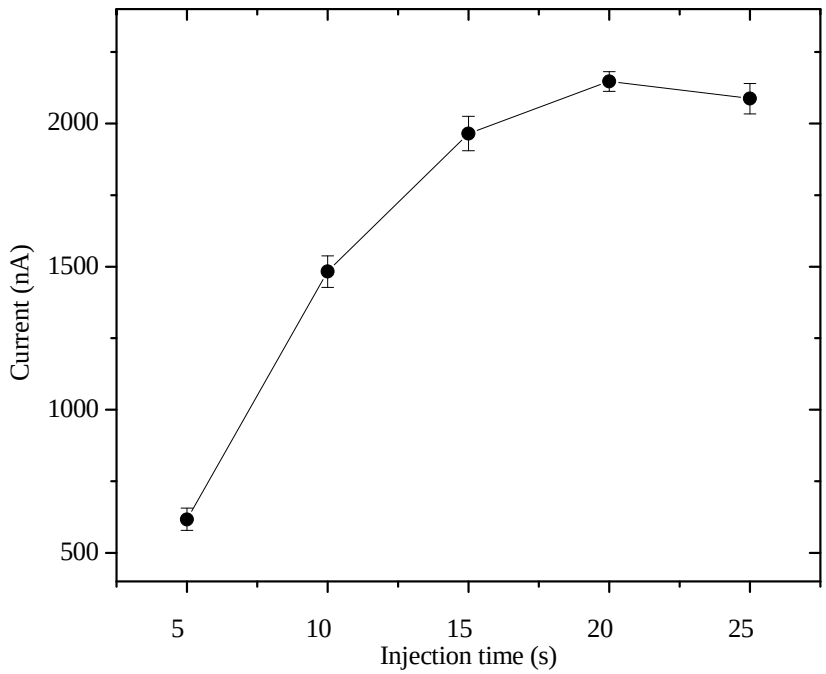

Figure 4.11 The effect of injection time on the migration time of 0.1 mM Cholesterol. Conditions: running buffer, a PB buffer (40 mM, pH 7.0) solution containing 0.68 $U \cdot mL^{-1}$; detection potential, +0.5 V, separation potential, +1600 V; injection potential, +450 V; at 25 µm Au wire working electrode.

4.2.8 Effect of interference

Figure 4.12 demonstrates the separation of 1 mM of cholesterol and 0.5 mM of ascorbic acid at the following detection potentials: +0.5 V, +0.6 V, and +0.8 V, respectively. Ascorbic acid was chosen as an interference agent in this work because it is generally found in serum. The results showed that the interference peak will be increased when the detection potential was increased. The peak current of ascorbic acid also increased when the detection potential was higher than +0.5 V. This indicated that using a detection potential of +0.5 V can reduce this interference effect.

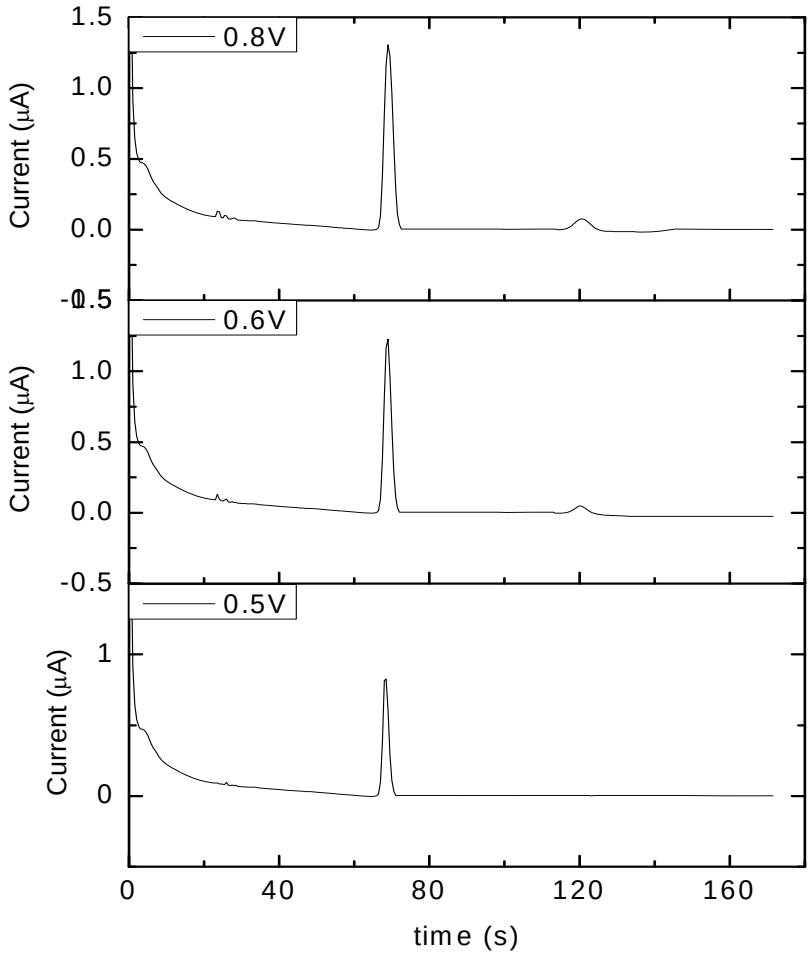

Figure 4.12 The effect of interference for PDMS Microchip capillary electrophoresis. The electropherogram of 1 mM of cholesterol and 0.5 mM ascorbic acid at different the detection potential, (a) +0.5 V, (b) +0.6 V, and (d) +0.8 V. Conditions: running buffer, a PB buffer (pH 7.0) solution containing 0.68 $U \cdot mL^{-1}$, separation potential, +1600 V; injection potential, +450 V; time, 20 s; at 25 μm Au wire working electrode.

4.2.9 Linear range and detection limit

The optimized conditions used for PDMS microchip capillary electrophoresis used as a 40 mM PB buffer solution (pH 7.0) containing 0.68 $U \cdot mL^{-1}$of the ChOx, a detection potential of +0.5 V, a separation voltage of +1600 V, and an injection time of 20s. Under the selected conditions, calibration curves were obtained in the range

of 38.7 μg·dL^{-1} (1 μM) to 270.6 mg·dL^{-1} (7 mM), with a coefficient of determination of 0.9984, as shown in Figure 4.13. The limit of detection (LOD) and limit of quantitation (LOQ) were found to be 38.7 ng·dL^{-1} (1 nM) and 38.7 μg·dL^{-1} (1 μM), respectively.

The expert panel [14] has suggested that the total blood cholesterol level found in an adult should be lower than 200 mg·dL^{-1} for normal blood cholesterol between 200 mg·dL^{-1} to 239 mg·dL^{-1} for borderline-high blood cholesterol, and higher than 240 mg.dL^{-1} for high blood cholesterol. Therefore, our proposed method can be applied for cholesterol level detection in real sample since all blood cholesterol levels are within the linear range.

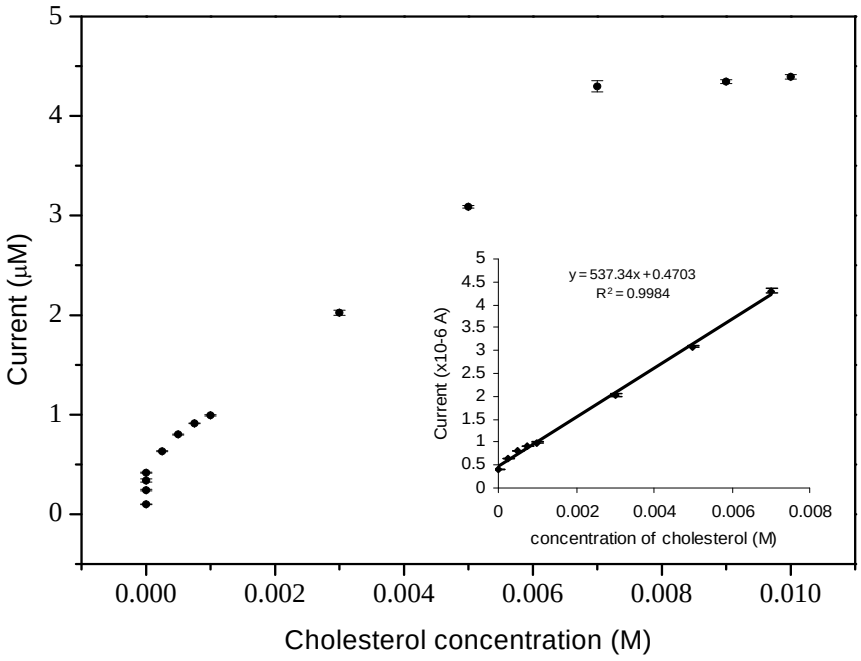

Figure 4.13 The calibration curve of cholesterol and linear range is shown in the insert Conditions: running buffer, a 40 mM PB buffer (pH 7.0) solution containing 0.68 U·mL^{-1}, separation potential, +1600 V; injection potential, +450 V; injection time, 20 s; at 25 μm Au wire working electrode.

4.2.10 Repeatability and Accuracy

In this experiment, the cholesterol standard was analyzed five times to determine the reproducibility of the peak current and migration time under the optimized conditions. The following optimized conditions were used 40 mM PB buffer (pH 7.0) containing 0.68 $U \cdot mL^{-1}$of the ChOx, a detection potential of +0.5 V, a separation voltage of +1600 V, and an injection time of 20 s. The average peak current, SD, and % RSD of cholesterol are shown in Table 4.1. The reproducibility of migration time, SD, and %RSD of cholesterol are shown in Table 4.2.

Table 4.1 The reproducibility of peak current for the detection of cholesterol (n=5).

Concentration (M)	**Peak current average (A)**	**SD**	**%RSD**
1 μM	0.42	0.012	2.85
500 μM	0.81	0.010	1.20
750 μM	0.91	0.005	0.53
1 mM	1.00	0.015	1.48
5 mM	3.13	0.063	2.01

Table 4.2 The reproducibility of migration time for the detection of cholesterol (n=5).

Concentration (M)	Migration time average (s)	SD	%RSD
1 μM	67.56	2.70	4.00
500 μM	69.86	1.56	2.23
750 μM	68.72	2.08	3.03
1 mM	69.05	2.22	3.22
5 mM	66.42	2.70	3.80

The relative standard deviations (RSD) of peak currents for 1 μM cholesterol, 500 μM cholesterol, 750 μM cholesterol, 1 mM cholesterol, and 5 mM cholesterol were 2.85 %, 1.20 %, 0.53 %, 1.48 %, and 2.01%, respectively. The RSD of migration time for 1 μM cholesterol, 500 μM cholesterol, 750 μM cholesterol, 1 mM cholesterol, and 5 mM cholesterol were 4.00 %, 2.23 %, 3.03 %, 3.22 %, and 3.80 %, respectively. Overall, this indicated that the proposed system exhibited an excellent performance both in the separation and detection of cholesterol for prolonged operation.

4.3 Sample analysis

Cholesterol is an important part of a healthy body because it is used to form cell membranes and some hormones; however, high levels of cholesterol in the blood can adhere to the walls of the arteries, thereby increasing the risk of coronary heart disease. Therefore, it is very important to quantify cholesterol in the blood. The determination of cholesterol in bovine serum was carried out under optimal conditions according to the procedures described above.

4.3.1 Analysis of cholesterol in lipid cholesterol from adult bovine serum

PDMS microchip capillary electrophoresis was used for the determination of cholesterol in bovine serum. The standard addition method was used to determine the amount of cholesterol in bovine serum. Figure 4.14 displays the results obtained from the determination of cholesterol in bovine serum by PDMS microchip. From these results, the relationship between the current response and the concentration of analyte under the selected condition was presented. The standard addition was investigated by spiking three difference standard cholesterol concentration (n=3) into the diluted bovine serum. The labeled concentrations of cholesterol in bovine serum were 20.0 $mg \cdot dL^{-1}$, 40.0 $mg \cdot dL^{-1}$, and 60.0 $mg \cdot dL^{-1}$, respectively. The cholesterol concentration in the bovine serum calculated from the standard addition curve, when using the proposed methodology, is shown in Table 4.3. Recoveries of 99.1 %-101.8 % were achieved, as shown in Table 4.3. These results indicated that the PDMS microchip capillary electrophoresis shows high specificity and sensitivity for real sample analysis.

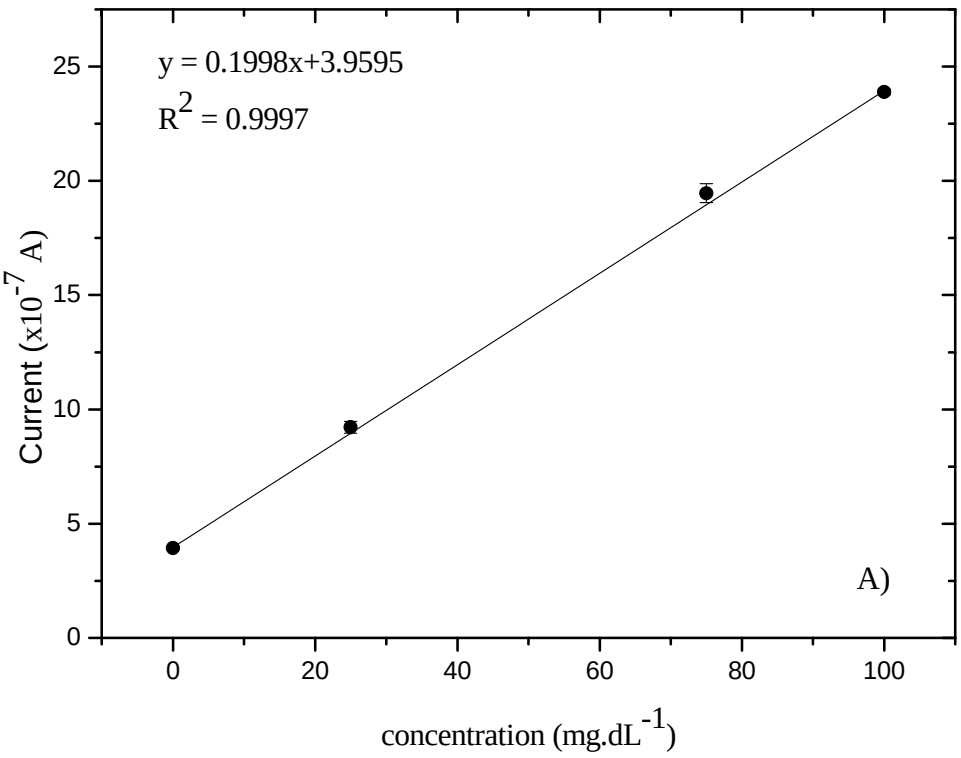
y = 0.1998x+3.9595
R2 = 0.9997
Current (x10-7 A)
concentration (mg.dL-1)
A)
0
5
10
15
20
25
0
20
40
60
80
100

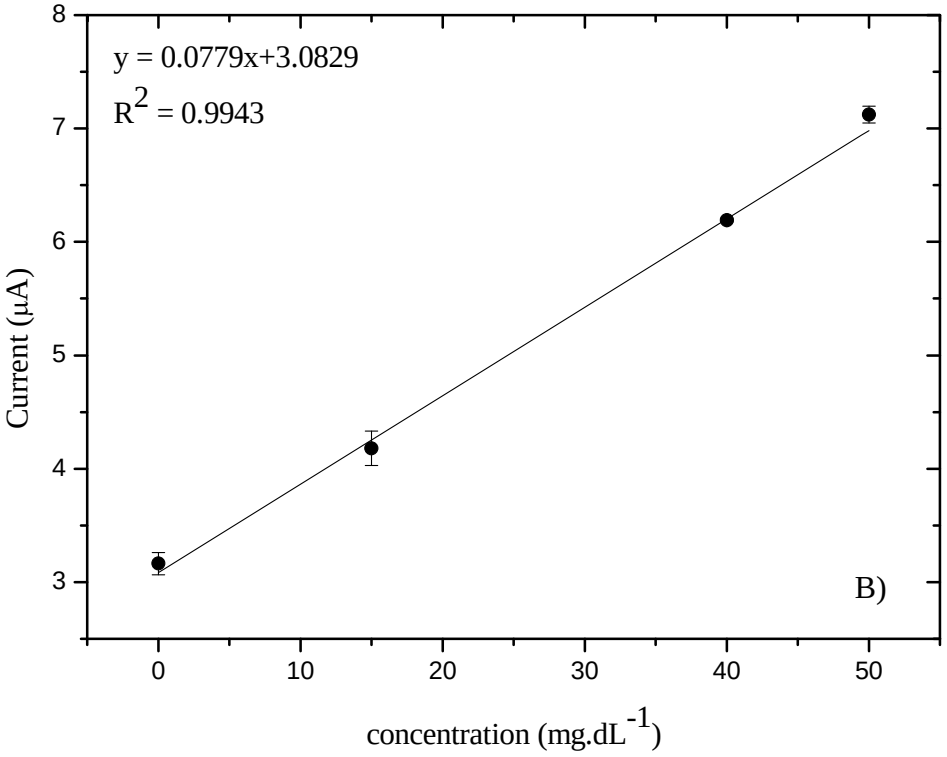
y = 0.0779x+3.0829
R2 = 0.9943
Current (µA)
concentration (mg.dL-1)
B)
3
4
5
6
7
8
0
10
20
30
40
50

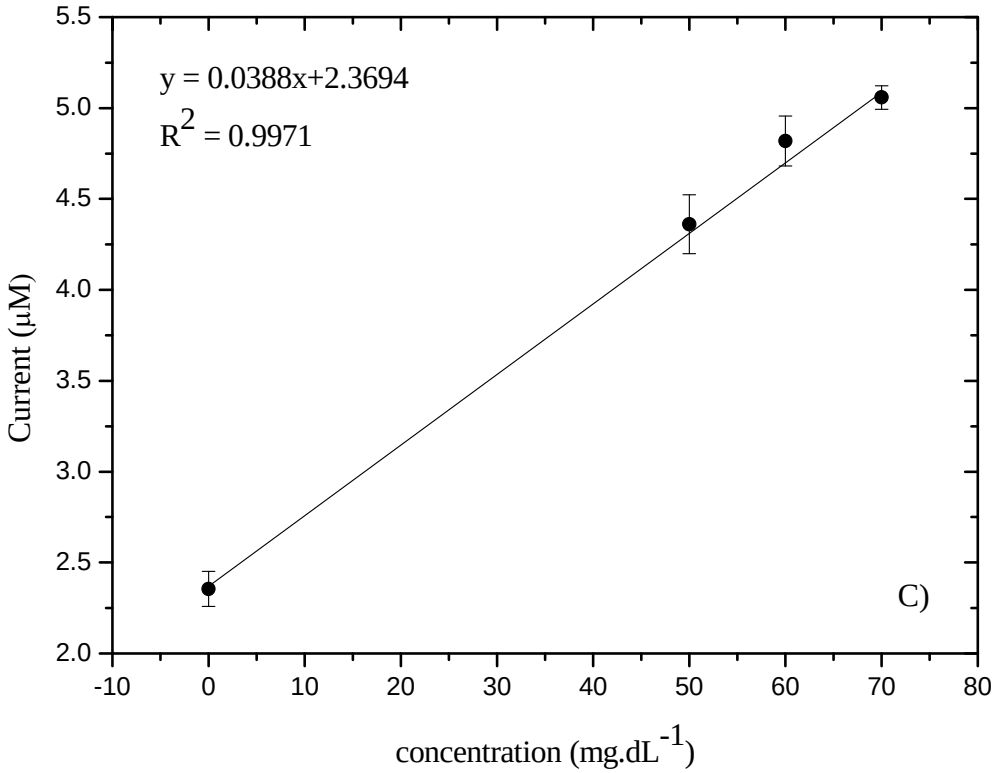

Figure 4.14 The relationship between the peak current and the concentration of cholesterol in bovine serum. The concentrations of cholesterol in bovine serum are A) 20 mg·dL^{-1}, B) 40 mg·dL^{-1}, C) 60 mg·dL^{-1}. Conditions: running buffer, a 40 mM PB buffer (pH 7.0) solution containing 0.68 U·mL^{-1}, separation potential, +1600 V; injection potential, +450 V; time, 20 s; at 25 μm Au wire working electrode.

Table 4.3 Results on the determination of cholesterol by the standard-addition method in a bovine serum sample (n=3).

Concentration of cholesterol in bovine serum sample ($mg \cdot dL^{-1}$)	**Determined value ($mg \cdot dL^{-1}$)**	**Relative error**	**% Recovery**
20.0	19.81	-0.95%	99.1
40.0	39.57	-1.07%	98.9
60.0	61.06	1.77%	101.8

CHAPTER V

CONCLUSIONS AND FUTURE PERSPECTIVES

5.1 Conclusions

In this thesis, an alternative approach to the rapid detection of cholesterol in serum using MCE fabricated from PDMS based on the coupling of enzymatic bioassays and amperometric detection, was developed. Electrochemical detection coupled with MCE enable selective and sensitive detection of electroactive analytes, while also simplifying the electropherograms. MCE is a potentially good alternative method because it is easy to use, requires small volumes of reagents and sample, and provides rapid analysis. In this method, EOF was used to flow sample and ChOx mixture. Cholesterol concentrations were measured by comparing the current response in the presence and absence of ChOx. The hydrogen peroxide product was detected at the gold wire working electrode. PDMS microchip capillary electrophoresis was first characterized by the separation of a mixed standard of dopamine and catechol prior to use.

The optimal conditions used were 40 mM phosphate buffer (pH 7.0), 0.68 $U \cdot mL^{-1}$ for the level of ChOx, +1600 V for the separation voltage, 20 s for the injection time, and +0.5 V for the detection potential of cholesterol. The calibration curve was linear from 38.7 $\mu g \cdot dL^{-1}$ (1 μM) to 270.6 $mg \cdot dL^{-1}$ (7 mM), with a coefficient of determination of 0.9984. PDMS microchip capillary electrophoresis gave a very low limit of detection (LOD) and limit of quantitation (LOQ); in fact, the LOD and LOQ were 38.7 $ng \cdot dL^{-1}$ (1 nM) and 38.7 $\mu g \cdot dL^{-1}$ (1 μM), respectively. The reproducibility of quantitative analysis for PDMS microchip is acceptable in terms of relative standard deviation. From these results, it can be conclude that PDMS microchip capillary electrophoresis based on the coupling of enzymatic bioassays and amperometric detection is a very rapid and sensitive method for the detection of cholesterol (within less than 100s). In addition, PDMS microchip capillary electrophoresis based on the coupling of enzymatic bioassays and amperometric

detection was also applied to measure cholesterol in a sample of bovine serum by standard addition methods.

From this measurement, the performance of the new microchip device was established for rapid and sensitive measurements of cholesterol. This ability to rapidly separate and quantitate cholesterol on a PDMS microchip capillary electrophoresis should find various application for clinical and biotechnological research fields.

REFERENCES

[1] National Heart, Lung and Blood Institute, National Institutes of Health, US Department of Health and Human Services. Detection, Evaluation and Treatment of High Blood Cholesterol in Adults (Adult Treatment Panel III) Final Report Third Report of the National Cholesterol Education Program. 5-11. Washington, D.C. Maryland: NIH Publication No. 02-5215, 2002.

[2] Goodman, D. S., Hulley, S. B., Clark, L. T., Davis, C. E., Fuster, V., LaRosa, J. C., Oberman, A. , Schaefer, E. J., Steinberg, D., Brown, W. V., Grundy, S. M., Becker, D., Bierman, E., Bochenek, J. S., Mullis, R., Stone, N., Hunninghake, D. B., Dunbar, J. M., Ginsberg, H. N., Illingworth, D. R., Sadin, H. C., Schonfeld, G., Cleeman, J. I., Brewer Jr, H. B., Ernst, N., Friedewald, W., Hoeg, J. M., Rifkind, B., and Gordon, D. Report of the national cholesterol education program expert panel on detection, evaluation, and treatment of high blood cholesterol in adults. Archives of International Medicine 148 (1988): 36-69.

[3] Arya, S. K., Prusty, A. K., Singh, S. P., Solanki, P. R., Pandey, M. K., Datta, M., and Malhotra B. D. Cholesterol biosensor based on N-(2-aminoethyl)-3-aminopropyl trimethoxysilane self-assembled monolayer. Analytical Biochemistry 363 (2007): 210-218.

[4] Dhand, C., Singh, S. P., Arya, S. K., Datta, M., and Malhotra, B. D. Cholesterol biosensor based on electrophoretically deposited conducting polymer film derived from nano-structured polyaniline colloidal suspension. Analytica Chimica Acta 602 (2007): 244-251.

[5] Khan, R., Kaushik, A., Solanki, R. P., Ansari, A. A., Pandey, K. M., and Malhotra, B. D. Zinc oxide nanoparticles-chitosan composite film for cholesterol biosensor. Analytica Chimica Acta 616 (2008): 207-213.

[6] Turkarslan, O., Kayahan, S. K., and Toppare, L. A new amperometric cholesterol biosensor based on poly (3,4-ethylenedioxypyrrole). Sensors and Actuators B-Chemical 136 (2009): 484-488.

[7] Belluzo, M. S., Ribone, M. E., and Lagier, C. M. Review Assembling Amperometric Biosensors for Clinical Diagnostics. Sensors 8 (2008): 1366-1399.

[8] Devadoss, A., and Burgess, J. D. Detection of Cholesterol through Electron Transfer to Cholesterol Oxidase in Electrode-Supported Lipid Bilayer Membranes. Langmuir 18 (2002): 9617-9621.

[9] Vidal, J.-C., Ruiz, E. G., and Castillo, J.-R. Design of a Multilayer Cholesterol Amperometric Biosensor for Preparation and Use in Flow Systems. Electroanalysis 13 (2000): 229-235.

[10] Vidal, J. C., GarcõÂa, E., and Castillo, J. R. In situ preparation of a cholesterol biosensor: entrapment of cholesterol oxidase in an overoxidized polypyrrole film electrodeposited in a flow system Determination of total cholesterol in serum. Analytica Chimica Acta 385 (1999): 213-222.

[11] Wang, J., Chatrathi, M. P., Tian, C., and Polsky, R. Microfabricated electrophoresis chips for simultaneous bioassays of glucose, uric acid, ascorbic acid, and acetaminophen. Analytical Chemistry 72 (2000): 2514-2518.

[12] Wang, J., and Chatrathi, M. P. Microfabricated electrophoresis chip for bioassay of renal markers. Analytical Chemistry 72 (2003): 525-529.

[13] Lee, H.-L., and Chen, S.-C. Microchip capillary electrophoresis with electrochemical detector for precolumn enzymatic analysis of glucose, creatinine, uric acid and ascorbic acid in urine and serum. Talanta 64 (2004): 750-757.

[14] Wang, J., Chatrathi, M. P., and Tian, B. Micromachined Separation Chips with a Precolumn eactor and End-Column Electrochemical Detector. Analytical chemistry 72 (2000): 5774-5778.

[15] Wang, J., and Chen, G. Microchip capillary electrophoresis with electrochemical detector for fast measurements of aromatic amino acids. Talanta 60 (2003): 1239-1244.

[16] Wang, J. Electrochemical detection for microscale analytical systems: a review. Talanta 56 (2002): 223-231

[17] Wu, Y., Lin, J. –M., Sua, R., Qua, F., and Cai, Z. An end-channel amperometric detector for microchip capillary electrophoresis. Talanta 64 (2004): 338–344.

[18] Holcomb, R. E., Kraly, J. R., and Henry, C. S. Electrode array detector for microchip capillary electrophoresis. Analyst 134 (2009): 486–492.

[19] Wong, I., and Ho, C. -M. Surface molecular property modifications for poly(dimethylsiloxane) (PDMS) based microfluidic devices. Microfluid Nanofluid 7 (2009): 291–306.

[20] Wang, A. -J., Xu, J. -J., and Chen, H. -Y. Proteins modification of poly(dimethylsiloxane) microfluidic channels for the enhanced microchip electrophoresis. Journal of Chromatography A 1107 (2006): 257–264.

[21] Mcdonald, J. C., and Whitesides, G. M. Poly(dimethylsiloxane) as a Material for Fabricating Microfluidic Devices. Accounts of Chemical Research 35 (2002): 491-199.

[22] Ping, G., Zhu, B., Jabasini, M., Xu, F., Oka, H., Sugihara, H., and Baba, Y. Analysis of Lipoproteins by Microchip Electrophoresis with High Speed and High Reproducibility. Analytical Chemistry 77 (2005): 7282-7287.

[23] Kim, J.-E., Cho, J.-H., and Paek, S.-H. Functional Membrane-Implanted Lab-on-a-Chip for Analysis of Percent HDL Cholesterol. Analytical Chemistry 77 (2005): 7901-7907.

[24] Götz, S., and Karst, U. Recent developments in optical detection methods for microchip separations. Analytical and Bioanalytical Chemistry 387 (2007) 183–192.

[25] Sueyoshi, K., Nagai, H., Wakida, S.-i., Nishii, J., Kitagawa, F., and Otsuka, K. Designing Multifunctional Microchips for Electrophoretic Analysis. Proceeding of Micro total analysis systems 1 (2004): 84-86

[26] Vickers, J. A., Dressen, B. M., Weston, M. C., Boonsong, K., Chailapakul, O., Cropek, D. M., and Henry, C. S. Thermoset polyester as an alternative material for microchip electrophoresis/electrochemistry. Electrophoresis 28 (2007): 1123–1129.

[27] Kricka, L. J. Microchips, microarrays, biochips and nanochips: personal laboratories for the 21st century. Clinica Chimica Acta 307 (2001): 219–223.

[28] Uchiyama, K., Nakajima, H., and Hobo, T. Detection methods for microchip separations. Analytical and Bioanalytical Chemistry 379 (2004): 375–382.

[29] García, C, D. and Henry, C. S. Direct Determination of Carbohydrates, Amino Acids, and Antibiotics by Microchip Electrophoresis with Pulsed Amperometric Detection. Analytical Chemistry 75 (2003): 4778–4783

[30] Geschke, O., Klank, H., and Telleman, P. Microsystem Engineering of Lab-on-a-chip Device. 1st ed., 1-7. Germany: Federal republic, 2004.

[31] Henry, C. S. Microchip Capillary Electrophoresis: method and protocols. 1-45. New Jersey: Humana Press Inc, 2006.

[32] Weinberger, R. Practical Capillary Elelctrophoresis. 1-421. New York: Academic Press, 2000.

[33] Karger, B. L. Capillary electrophoresis. Biotechnology 3 (1992): 59-64.

[34] Novotny, M. V. Capillary electrophoresis. Biotechnology 7 (1996): 29-34.

[35] Kirby, B. J. Micro- and Nanoscale Fluid Mechanics for Engineers: Transport in Microfluidic Devices. [online]. Available from: http://www.kirbyresearch.com/index.cfm/wrap/textbook/microfluidicsnanofluidics.html, 2009. [2009, 10 20]

[36] Weston, A., and Brown, P. R. HPLC and CE Principles and Practice. California: Academic Press, 1997.

[37] Shihabi, Z. K.. Stacking in capillary zone electrophoresis. Journal of Chromatography A 902 (2000): 107–117.

[38] Quirino, J. P., and Terabe, S. Sample stacking of cationic and anionic analytes in capillary electrophoresis. Journal of Chromatography A 902 (2000): 119-135.

[39] Bagotsky, V. S. Fundamentals of electrochemistry. New Jersey: John Wiley & Sins, 2006.

[40] Eggins, B. Biosensors: An Introduction. New York: John Wiley & Sons, 1996.

[41] Monk, S. Fundametals of Electroanalytical Chemistry. New York: John Wiley & Sons, 2001.

[42] Wang, J. Analytical Electrochemistry. New York: John Wiley & Sons, 1994.

[43] Sawyer, D. T. Experimental Electrochemistry for Chemists. New York: John Wiley & Sons, 1974.

[44] Zoski, C. G. Handbook of electrochemistry. UK: Elsevier, 2006.

[45] Hadd, A. G., Jacobson, S. C., and Ramsey J. M. Microfluidic assays of acetylcholinesterase inhibitors. Analytical Chemistry 71 (1999): 5206-5212

[46] Harrison, D. J., Fluri, K., Seiler, K., Fan, Z. H., Effenhauser, C. S., and Manz, A. Micromachining a Miniaturized Capillary Electrophoresis- Based Chemical Analysis System on a Chip. Science 261(1993): 895-897.

[47] Li, P. C. H., Harrison, and D. J. Transport, manipulation, and reaction of biological cells on chip using electrokinetic effects. Analytical Chemistry 69 (1997): 1564-1568.

[48] Hadd, A. G., Raymond, D. E., Haliwell, J. W., Jacobson, S. C., and Ramsey, S. C. Microchip device for performing enzyme assays. Analytical Chemistry 69 (1997): 3407-3412.

[49] Lagally, E. T., Medintz, I., and Mathies, R. A. Single-molecule DNA amplification and analysis in an integrated microfluidic device. Analytical Chemistry 73 (2001): 565-570.

[50] Khandurina, J., McKnight, T. E., Jacobson, S. E., Waters, L. C., Foote, R. S., and Ramsey, J. M. Integrated systems for rapid PCR-based DNA analysis and microfluidic devices. Analytical Chemistry 72 (2000): 2995-3000.

[51] Eteshola, E., and Leckband, D. Development and Characterization of an ELISA Assay in PDMS Microfluidic Channels. Sensors & Actuators B 72 (2001): 129-133.

[51] Wang, J., Ibanez, A., Chatrathi, M. P., and Escarpa, A. Electrochemical enzyme immunoassay on microchip platforms. Analytical Chemistry 73 (2001): 5323-5327.

[52] Unger, M. A., Chou, H.-P., Thorsen, T., Scherer, A., and Quake, S. R. Monolithic microfabricated valves and pumps by multilayer soft lithography. Science 288 (2000): 113-116.

[53] Mcdonald, J. C., and Whitesides, G. M. Poly(dimethylsiloxane) as a Material for Fabricating Microfluidic Devices. Accounts of Chemical Research 35 (2002): 491-499.

[54] Cuchel, M., Bloedon, L. T., Szapary, P. O., Kolansky, D. M., Wolfe, M. L., Sarkis, A., Millar, J. S., Ikewaki, K., Siegelman, E. S., Gregg, R. E., and Rader, D. J. Inhibition of microsomal triglyceride transfer protein in familial

hypercholesterolemia. The New England Journal of Medicine 356 (2007): 148–156.

[55] Wedro, B., and Kulick, D. Lowering Your Cholesterol. [online]. Available from: http://www.medicinenet.com/cholesterol/article.htm, 2010. [2010, 01 27]

VITAE

Name: Miss Nipapan Ruecha

Date and place of birth: 12 May 1985

Place of birth: Bangkok, Thailand

Education: 2009-2007 Chulalongkorn University, postgraduate study leading to a Master of Science degree program in Petrochemistry and Polymer Science

2006-2002 Kasetsart University, Bachelor of Science (General Science)

Home address: 34/187 Moo.11 Bangkruai-sainoi Rd., Sainoi, Nontaburi, 11150, Thailand

E-mail: lookchin_bank@hotmail.com